Calhoun: The NPS Institutional Archive

DSpace Repository

Theses and Dissertations | 1. Thesis and Dissertation Collection, all items

2003-09

Maximizing the stability of an ensemble of clocks

Ruiz Perez, Juan Jose

Monterey, California. Naval Postgraduate School

Copyright is reserved by the copyright owner.

Downloaded from NPS Archive: Calhoun

http://www.nps.edu/library

Calhoun is the Naval Postgraduate School's public access digital repository for research materials and institutional publications created by the NPS community. Calhoun is named for Professor of Mathematics Guy K. Calhoun, NPS's first appointed -- and published -- scholarly author.

Dudley Knox Library / Naval Postgraduate School
411 Dyer Road / 1 University Circle
Monterey, California USA 93943

NAVAL POSTGRADUATE SCHOOL
Monterey, California

THESIS

MAXIMIZING THE STABILITY OF AN ENSEMBLE OF CLOCKS

by

Juan J. Ruiz

September 2003

Thesis Advisor: Alan Washburn
Second Reader: Paul Sánchez

Approved for public release; distribution is unlimited

THIS PAGE INTENTIONALLY LEFT BLANK

REPORT DOCUMENTATION PAGE			Form Approved OMB No. 0704-0188
Public reporting burden for this collection of information is estimated to average 1 hour per response, including the time for reviewing instruction, searching existing data sources, gathering and maintaining the data needed, and completing and reviewing the collection of information. Send comments regarding this burden estimate or any other aspect of this collection of information, including suggestions for reducing this burden, to Washington headquarters Services, Directorate for Information Operations and Reports, 1215 Jefferson Davis Highway, Suite 1204, Arlington, VA 22202-4302, and to the Office of Management and Budget, Paperwork Reduction Project (0704-0188) Washington DC 20503.			
1. AGENCY USE ONLY *(Leave blank)*	**2. REPORT DATE** September 2003	**3. REPORT TYPE AND DATES COVERED** Master's Thesis	
4. TITLE AND SUBTITLE **Maximizing the Stability of an Ensemble of Clocks**			**5. FUNDING NUMBERS**
6. AUTHOR(S) Juan J. Ruiz			
7. PERFORMING ORGANIZATION NAME(S) AND ADDRESS(ES) Naval Postgraduate School Monterey, CA 93943-5000			**8. PERFORMING ORGANIZATION REPORT NUMBER**
9. SPONSORING /MONITORING AGENCY NAME(S) AND ADDRESS(ES) N/A			**10. SPONSORING/MONITORING AGENCY REPORT NUMBER**
11. SUPPLEMENTARY NOTES The views expressed in this thesis are those of the author and do not reflect the official policy or position of the Department of Defense or the U.S. Government.			
12a. DISTRIBUTION / AVAILABILITY STATEMENT Approved for public release; distribution is unlimited			**12b. DISTRIBUTION CODE**

13. ABSTRACT ***(maximum 200 words)***

Atomic Clocks provide "stable" signals that are mainly used to generate time scales and to measure differences of time between events. Each atomic clock can individually be characterized according to the stability of the scale it produces.

Due to the stochastic behavior of each clock, usually clock ensembles are used to build more stable time scales. This process requires basically two steps. First it is required to individually characterize each time source to identify the particular noise components present. Second, a measure of performance is required in order to derive an algorithm based on it to properly "weigh" this particular clock in the process of creating a combined scale.

In this thesis both problems are faced using an operations research approach: each clock is modeled, analyzed and characterized by a time-dependent measure of performance related to its intrinsic stability, and optimally combined to produce a more stable combined time scale. The optimality criterion is directly related to the spectral characteristics of the noise sources present.

14. SUBJECT TERMS Characterization of Atomic Clocks, Frequency Stability, Allan variance			**15. NUMBER OF PAGES** 103
			16. PRICE CODE
17. SECURITY CLASSIFICATION OF REPORT Unclassified	**18. SECURITY CLASSIFICATION OF THIS PAGE** Unclassified	**19. SECURITY CLASSIFICATION OF ABSTRACT** Unclassified	**20. LIMITATION OF ABSTRACT** UL

NSN 7540-01-280-5500 Standard Form 298 (Rev. 2-89)
Prescribed by ANSI Std. 239-18

THIS PAGE INTENTIONALLY LEFT BLANK

Approved for public release; distribution is unlimited

MAXIMIZING THE STABILITY OF AN ENSEMBLE OF CLOCKS

Juan José Ruiz Pérez
Lieutenant Commander, Spanish Navy
B.A., Spanish Naval Academy, 1985

Submitted in partial fulfillment of the
requirements for the degree of

MASTER OF SCIENCE IN OPERATIONS RESEARCH

from the

NAVAL POSTGRADUATE SCHOOL
September 2003

Author: Juan J. Ruiz

Approved by: Professor Alan Washburn
Thesis Advisor

Professor Paul Sánchez
Second Reader

James N. Eagle
Chairman, Department of Operations Research

THIS PAGE INTENTIONALLY LEFT BLANK

ABSTRACT

Atomic Clocks provide "stable" signals that are mainly used to generate time scales and to measure differences of time between events. Each atomic clock can individually be characterized according to the stability of the scale it produces.

Due to the stochastic behavior of each clock, usually clock ensembles are used to build more stable time scales. This process requires basically two steps. First it is required to individually characterize each time source to identify the particular noise components present. Second, a measure of performance is required in order to derive an algorithm based on it to properly "weigh" this particular clock in the process of creating a combined scale.

In this thesis both problems are faced using an operations research approach: each clock is modeled, analyzed and characterized by a time-dependent measure of performance related to its intrinsic stability, and optimally combined to produce a more stable combined time scale. The optimality criterion is directly related to the spectral characteristics of the noise sources present.

Real laboratory data provided by the “Real Observatorio de la Armada”, ROA (Royal Observatory of the Spanish Navy) is used to tune the final algorithm to the time standards present in the ROA.

THIS PAGE INTENTIONALLY LEFT BLANK

TABLE OF CONTENTS

I. INTRODUCTION. CHARACTERIZATION OF CLOCKS AND OSCILLATORS....1
A. INTRODUCTION....1
B. CLOCK MODEL AND DEFINITIONS....3
C. CLASSIFICATION OF NOISE PROCESSES....5
D. TIME DOMAIN CHARACTERIZATION, THE ALLAN VARIANCE....8
1. Definition and Estimate....8
2. A Simple Example to Compute Allan Variance....15
3. Confidence Intervals for the Allan Variance....18
4. Time – Frequency Duality....20

II. CHARACTERIZATION OF THE CLOCK ENSEMBLE....23
A. STATEMENT OF THE PROBLEM....23
B. CONSTRUCTING A COMPOSITE CLOCK....24
C. MATHEMATICAL FORMULATION....26
D. CONSIDERATIONS ON THE COVARIANCE MATRICES *R* AND *S*....31
1. Relationship Between the Matrices *R* and *S*....32
2. A Simple Case with an Ensemble of *K*=3 clocks....34
3. Selection of the Free (Co)variances r_{13}, r_{23} and r_{33}....35
4. The Classical Three-Cornered Hat Method....37
5. Optimal Selection of the Free Covariances: Constrained or Unconstrained Minimization?....38
6. New Proposal for the Constrained Minimization Problem....39
7. Mathematical Formulation of the Minimization Problem....40
E. ESTIMATION OF THE COVARIANCE MATRICES *R* AND *S*....42
1. Notation and Definitions....42
2. Estimation of Allan (Co)variances from the Measured Data....43

III. COMPARISON, TESTING AND SIMULATION....45
A. OVERVIEW....45
1. Description of the Different Tests Performed....45
2. Analysis of the Uniform Random Number Generator....46
3. Definition of Proposed Measures of Performance (*MOP*)....46
B. TEST N°1, SINGLE POINT COMPARISON....47
C. TEST N°2, RANDOM COVARIANCE MATRIX SIMULATION....50
D. TEST N°3, TEST OF SENSITIVITY OF THE NEW PROPOSAL....54
E. TEST N°4, PHASE SIMULATION....59
1. Generation of the Appropriate Type of Noise Process....59
2. Generation of the Fractional Frequency Deviations and Time Differences Between Pairs of Clocks....62

3. Estimation of the Relative Covariance Matrix *S* Associated with the Ensemble 65
4. Estimation of the Absolute Covariance matrix *R* Associated with the Ensemble 68
5. Estimation of the Weights Associated with Each Clock. 69

IV. APPLICATION OF THE METHOD TO REAL DATA 71
A. OVERVIEW 71
B. INITIAL EXPLORATION OF THE DATA 71
C. INITIAL FILTERING 72
D. CHARACTERIZATION OF THE ENSEMBLE 74

CONCLUSIONS 77

LIST OF REFERENCES 79

INITIAL DISTRIBUTION LIST 83

LIST OF FIGURES

Figure 1. Deterministic frequency and time deviations 6
Figure 2. Ratio of sample /Allan variance for different noise processes (After ref. [10])....11
Figure 3. Sample data to compute Allan variance....15
Figure 4. Comparison of 1st *MOP* 52
Figure 5. Comparison of 2nd *MOP* 52
Figure 6. Comparison of 3rd *MOP*....53
Figure 7. Simulated vs. Computed Allan variances 56
Figure 8. Simulated vs. Computed Optimal Weights....56
Figure 9. Relative errors in Allan variances and Weights....58
Figure 10. Simulated noise processes and corresponding Allan deviation plot....61
Figure 11. Simulated noise processes and corresponding Power Spectral Density plot...62
Figure 12. Absolute Fractional Frequency fluctuations 63
Figure 13. Absolute Time differences....64
Figure 14. Relative Fractional Frequency fluctuations 64
Figure 15. Relative Time differences....65
Figure 16. Diagonal terms of matrix $\boldsymbol{S}$....66
Figure 17. Off-diagonal terms of matrix $\boldsymbol{S}$....67
Figure 18. Diagonal terms of matrix $\boldsymbol{R}$....68
Figure 19. Simulated vs. computed weights....69
Figure 20. Raw Time differences between clocks 72
Figure 21. Filtered Time differences between clocks 73
Figure 22. Filtered Fractional frequency between clocks 73
Figure 23. Computed Allan deviation for the ensemble 74
Figure 24. Computed Allan deviation (Three Cornered Hat) 75

THIS PAGE INTENTIONALLY LEFT BLANK

LIST OF TABLES

Table 1. Noise processes used in modeling frequency instability (frequency).....8
Table 2. Relationship between classical standard deviation and Allan deviation (After ref. [18]) 12
Table 3. Steps for computing Allan deviation for $\tau = 1s$ 16
Table 4. Steps for computing Allan deviation for $\tau = 2s$ 17
Table 5. Steps for computing (overlapped) Allan deviation for $\tau = 2s$ 18
Table 6. Values of κ_α to compute confidence intervals for σ_y^2 19
Table 7. Empirical expressions for the degrees of freedom of overlapped Allan variance (After ref. [3]).....20
Table 8. Noise processes used in modeling frequency instability (Time) 21
Table 9. Comparison of the covariance and correlation matrices for the five approaches.....49
Table 10. Comparison of the *MOP*'s obtained by each method 50
Table 11. Summary table for *MOP* 1 53
Table 12. Summary table for *MOP* 2 54
Table 13. Summary table for *MOP* 3 54
Table 14. Summary of relative errors in Allan variance.....57
Table 15. Summary of relative errors in Weights.....57
Table 16. Noise processes used in modeling frequency instability 60
Table 17. Theoretical and computed slopes for the different noise processes.....61
Table 18. Structure of the data file.....71

THIS PAGE INTENTIONALLY LEFT BLANK

ACKNOWLEDGMENTS

The author wants to thank The Royal Observatory of the Spanish Navy (ROA) for the help and laboratory data provided to perform this study.

The author also wants to thank specially Dr. Juan Palacio, Dept. Head of the Time Section (ROA) and Dr. Javier Galindo (ROA), Dept. Head of Time Laboratory for the great help provided and fruitful conversations maintained during these last two years.

THIS PAGE INTENTIONALLY LEFT BLANK

EXECUTIVE SUMMARY

Atomic Clocks provide "stable" signals that are mainly used to generate time scales and to measure differences of time between events. Each atomic clock can individually be characterized according to the stability of the scale it produces.

Due to the stochastic behavior of each clock, usually clock ensembles are used to build more stable time scales. This process requires basically two steps. First it is required to individually characterize each time source to identify the particular noise components present. Second, a measure of performance is required in order to derive an algorithm based on it to properly "weigh" this particular clock in the process of creating a combined scale.

In this thesis both problems are faced using an operations research approach: each clock is modeled, analyzed and characterized by a time-dependent measure of performance related to its intrinsic stability, and optimally combined to produce a more stable combined time scale. The optimality criterion is directly related to the spectral characteristics of the noise sources present.

The thesis has been divided in four main sections with the following contents:

Section one is a general introduction of the problem of characterization of clocks and precision oscillators. The theory of analysis of stability and the physical magnitudes involved in this process are also presented.

The different kinds of noise processes that may be present in precision oscillators are outlined and their intrinsic characteristics in the frequency and time domains are also introduced as background theory.

Special attention is given to the main statistic used in frequency stability: the Allan variance. The need of a new estimator to analyze the time series of measurement data is shown and illustrated.

In section two, the complete characterization problem is presented as a nonlinear optimization problem subjected to nonlinear constraints. The computation of weights to assign to each clock with the objective of finding a composite time scale is also addressed.

Classical approaches are presented and a new approach is outlined.

In chapter three, simulation is used to test and compare the various approaches. Four different tests are carried out:

- A single point simulation for a hypothetical case that has been analyzed previously
- Random generation of covariance matrices
- A test of sensitivity carried out on the new proposal to check if small changes in the input parameters lead to coherent results
- Finally, a complete simulation involving the generation of time difference data under the presence of noise is performed. The importance of the length of the time series is addressed.

Finally, in section four, the method is applied to real data provided by the Royal Observatory of the Spanish Navy. A complete characterization of an ensemble of five atomic clocks is performed.

THIS PAGE INTENTIONALLY LEFT BLANK

I. INTRODUCTION. CHARACTERIZATION OF CLOCKS AND OSCILLATORS

A. INTRODUCTION

Precision oscillators play an important role in many aspects of our daily life. High-speed communications, space tracking, navigation and many other important applications are based on a precise and accurate synchronization among the different devices and the equipment that is involved in such activities. In this chapter, the basic concepts and definitions required for characterization and analysis of frequency stability of general precision oscillators is briefly described.

Clocks are the instruments we use to measure time or, to be more precise, increments of time elapsed since an arbitrary chosen initial reference. Basically, every clock consists of two different parts: an oscillating device and a counter that accumulates the number of oscillations performed since it is initially set to zero. Thus, the initial reference of "time" is somewhat arbitrary. Clocks have evolved from astronomical clocks based on planetary movements and governed by the laws of celestial mechanics to clocks based on pendulums, mechanical springs, or the piezoelectric properties of quartz crystals. Precision atomic clocks used today are based on the quantum transitions of electrons occurring between the different states of certain elements like rubidium or cesium [1].

The initial definition of the second is based on the mean solar day, which has exactly 86400 seconds. The definition of the mean solar day is based on astronomical computations. As new precise instruments were available to measure increments of time, it was soon noticed that there were irregularities in the rotation of the Earth; in particular, the speed of rotation was observed to be slowing down at a rate in the order of one second per year. It was not until 1960 in the 11^{th} General Conference on Weights and

Measures (CGPM, *Conférence Générale des Poids et Mesures*) when a new definition based on the tropical year and proposed by the International Astronomical Union was adopted. Finally, in 1967 in the 13th General Conference on Weights and Measures the definition based on astronomical theories was abandoned. A new definition based on the physical properties of a particular isotope of cesium was adopted and confirmed in 1997 by the International Committee for Weights and Measures (CIPM, *Comité International des Poids et Mesures*). The new definition was:

> The second is the duration of 9 192 631 770 periods of the radiation corresponding to the transition between the two hyperfine levels of the ground state of the cesium 133 atom.

Even atomic clocks based on cesium present differences in the time scale that each clock generates. Their readings are different, and the time they take to perform a complete oscillation is different from oscillation to oscillation and from clock to clock. The objectives in this thesis include the study of the different behavior of atomic clocks in order to assign them a measure of performance indicating how well each clock is performing. This measure of performance associated with each clock can later be used as a weighting factor to build a new composite time scale derived from the data supplied from the clocks belonging to the ensemble.

These weighting factors are time varying numbers that contain information of the goodness of the scale generated for each clock. The more stable the frequency generated by a clock, the more weight this clock will have in the composite scale. The fact that there is no reference to compare to and that the only available data are relative measures among real clocks of similar characteristics make this problem interesting as well as challenging [2].

B. CLOCK MODEL AND DEFINITIONS

Every atomic clock provides as outputs different electronic signals, some of them are digital signals with square pulses, while some are continuous like the sinusoidal signals of different frequencies (generally 1, 5 and 10 MHz) that can be represented according to the following model [3,4]:

$$V(t) = V_0(t) \cdot \sin(\Phi(t)) \tag{1.1}$$

Here $V(t)$ represents the voltage level of the signal, $V_0(t)$ represents the magnitude or amplitude of the oscillations and $\Phi(t)$ is the total oscillator phase, starting from some arbitrary origin $\Phi(t=0)$. We will assume that the amplitude $V_0(t)$ for atomic clocks can be treated as a constant V_0.

The *total oscillator phase* $\Phi(t)$ can be decomposed as the sum of a purely deterministic component that is responsible for the oscillation at a fixed *nominal frequency* ν_0, plus a stochastic component known as the *residual phase* or *phase deviation* $\phi(t)$:

$$\Phi(t) = 2 \cdot \pi \cdot \nu_0 \cdot t + \phi(t) \tag{1.2}$$

The *instantaneous angular frequency* $\omega(t)$ of the oscillations is defined as the time derivative of the total oscillator phase:

$$\omega(t) = \frac{d}{dt}\Phi(t) = \frac{d}{dt}\left(2 \cdot \pi \cdot \nu_0 \cdot t + \phi(t)\right) = 2 \cdot \pi \cdot \nu_0 + \dot{\phi}(t) \tag{1.3}$$

Finally, the *instantaneous frequency* $\nu(t)$ is defined as:

$$\nu(t) = \frac{1}{2 \cdot \pi}\omega(t) = \nu_0 + \frac{\dot{\phi}(t)}{2 \cdot \pi} \tag{1.4}$$

This quantity can be considered as a nominal frequency of oscillation ν_0 affected by the perturbation term $\dot{\phi}(t)/(2 \cdot \pi)$. This is the quantity we are interested in, since it

defines the stability of a clock. The instantaneous frequency of the oscillations $\nu(t)$ may change erratically because of the processes involved in the generation of the signal inside the clock and also because of external factors (environmental, geographic, etc.). Unfortunately, since infinite bandwidth measurements are not possible, an exact value for the instantaneous frequency is not measurable.

The statistical quantity that is used in stability characterizations of oscillators is an adimensional quantity that measures the relative instantaneous deviation in frequency from its nominal or predefined value ν_0. It is called the *fractional frequency* or *fractional frequency fluctuation* and is defined as

$$y(t) = \frac{\nu(t) - \nu_0}{\nu_0} = \frac{\dot{\phi}(t)}{2 \cdot \pi \cdot \nu_0} \tag{1.5}$$

For the same reason given above related to the need of infinite bandwidth, it is not possible to measure the instantaneous fractional frequency, but, as will be shown, an average value can be directly estimated from differences in time between clocks.

The *time deviation* $x(t)$ is defined as the integral of the fractional frequency with respect to time. It has dimensions of time and represents the difference in time between two clocks or the time difference between a real clock and an ideal one oscillating exactly with a frequency of ν_0 and initially synchronized at time $t = 0$. This is the magnitude that is measured in time laboratories and used to estimate the average fractional frequency.

$$x(t) = \int_0^t y(t) \cdot dt = \frac{\phi(t)}{2 \cdot \pi \cdot \nu_0}, \quad y(t) = \frac{dx(t)}{dt} = \frac{\dot{\phi}(t)}{2 \cdot \pi \cdot \nu_0} \tag{1.6}$$

Time deviation $x(t)$ and phase deviation $\phi(t)$ are linearly related and consequently present the same spectral characteristics.

C. CLASSIFICATION OF NOISE PROCESSES

The fractional frequency deviation $y(t)$, the time deviation $x(t)$ or the phase deviation $\phi(t)$ are all affected by two different categories. First, there is a systematic or deterministic component that is generally produced by two situations [5,6]:

- A constant frequency of oscillation that is different than the nominal value ν_0.
- A constant *frequency drift D*, when the frequency of a clock instead of being constant changes linearly with time.

The second category is caused by random processes involved inside the clocks. This is the most difficult category to characterize the time scale generated by each clock, since, even if the frequency of the clock is changing, as long as it changes according to a deterministic or predefined pattern, the scale can always be compensated by algebraic manipulations. On the other hand, the random effects are more difficult to measure and compensate. Study of these effects constitutes the central part of this work.

For a clock presenting an initial frequency offset and a constant drift, the time deviation can be expressed as [5]:

$$x(t) = x_0 + y_0 \cdot t + \frac{1}{2} D \cdot t^2 + \varepsilon(t) \tag{1.7}$$

Here x_0 is the synchronization error, and y_0 is the fractional frequency offset and includes the effects produced by an initial frequency of oscillation different than the nominal ν_0 at time $t = 0$. The term involving the drift rate D includes the effects of a linear rate of change in the instantaneous frequency of oscillation $\nu(t)$ and $\varepsilon(t)$ represents the random effects. In Figure 1, the effect of frequency offset and frequency drift in the quantities $x(t)$ and $y(t)$ is shown. In the figure, the two systematic error cases are presented: a

clock with a constant frequency but different than the nominal ν_0 and another clock with a negative frequency drift. The effects produced by environmental fluctuations, humidity, temperature, shock, vibrations, radiation etc., can also induce other types of systematic deviations (i.e. modulation sidebands) that will not be treated here [5,6].

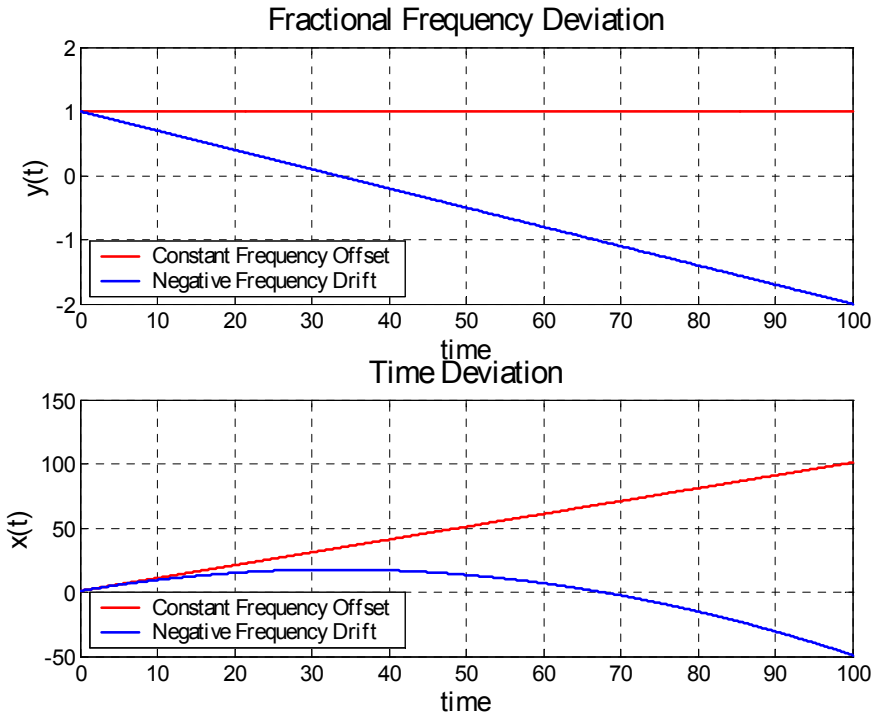

Figure 1. Deterministic frequency and time deviations

The types of noise present in atomic clocks are classified according to their spectral characteristics. In the frequency domain, power-law spectral densities serve as a reasonable and accurate model of the random fluctuations in precision oscillators. In practice, these random fluctuations are often represented by the sum of five such noise processes assumed to be independent, as [3,7,8]:

$$S_y(f) = \begin{cases} \sum_{\alpha=-2}^{\alpha=2} h_\alpha \cdot f^\alpha & 0 < f < f_h \\ 0 & f > f_h \end{cases} \tag{1.8}$$

Where $S_y(f)$ is the power spectral density (PSD) of the fractional frequency, h_α is a constant associated with each noise type and f_h is the high frequency cut off frequency. $S_y(f)$ is proportional to the squared magnitude of the Fourier Transform of the fractional frequency.

The duality time-frequency and the relationships in the time domain among the fractional frequency $y(t)$, time deviation $x(t)$ or phase deviation $\phi(t)$ have a counterpart in the frequency domain, so it is frequent to find in the literature equivalent expressions for the noise models as a function of the power spectral densities of the time deviation $S_x(f)$ or the phase deviation $S_\phi(f)$. All of them are equivalent. The dual relationships of (1.6) in the frequency domain are [9]:

$$S_x(f) = \frac{1}{\left(2 \cdot \pi \cdot \nu_0\right)^2} S_\phi(f), \quad S_y(f) = \frac{f^2}{\nu_0^2} S_\phi(f) \tag{1.9}$$

The noise processes present are usually identified by plotting in logarithmic axes the PSD and then fitting a first degree polynomial. The corresponding slope of the straight line relates it to the noise type.

Table 1 summarizes five commonly used models for noise and their characterizations in the frequency domain [3,6,10]:

Noise Process	Frequency Domain	
	$S_y(f)$	$S_x(f)$ or $S_\phi(f)$
Slope: $\log(PSD)\ vs.\ \log(f)$ α, β	α	β
Random Walk Frequency Modulation	-2	-4
Flicker Frequency Modulation	-1	-3
White Frequency Modulation	0	-2
Flicker Phase Modulation	1	-1
White Phase Modulation	2	0

Table 1. Noise processes used in modeling frequency instability (frequency)

D. TIME DOMAIN CHARACTERIZATION, THE ALLAN VARIANCE

1. Definition and Estimate.

The quantity of interest is the fractional frequency, or to be more precise, the residual fractional frequency which corresponds to the same concept once the deterministic components or systematic effects have been removed [10,11].

The fractional frequency data provides information about the instantaneous frequency of the oscillator. If it has a non zero but nearly constant value, it means that the oscillator is generating a nearly constant (stable) signal but at a frequency different than the nominal ν_0 at which it is supposed to oscillate. This is not a bad sign as long as it has little variation. The parameter that characterizes the stability is consequently a function of the variability of the fractional frequency $y(t)$.

The instantaneous value of the fractional frequency of one clock compared to another cannot be computed, but an average value during a time interval can be obtained from the time differences between these clocks. Let us suppose that $x(t)$ represents the time difference between two clocks at time *t*. We usually compare the clocks at equally spaced instants of time, that is, the values of $x(t)$ known to us are $x_m \equiv x(m \cdot \tau_0)$ where *m* takes integer values and τ_0 represents the time spacing or sample period between measurements. The time series containing the measurement of time differences is represented by $\{x_0, x_1, x_2, x_3, ..., x_{N-1}\}$, where *N* is the number of time difference data points available.

The relationship between the fractional frequency and the time difference is introduced in (1.6); average values of fractional frequency $\overline{y}(t)$ can be estimated by approximating the derivative with the ratio of increments:

$$y(t) = \frac{dx(t)}{dt}$$
$$\overline{y}(t) = \frac{\Delta x(t)}{\Delta t} = \frac{x(t+\tau) - x(t)}{\tau} \tag{1.10}$$

During periods of time of τ_0 seconds, average values for $y(t)$ can be computed:

$$\overline{y}(0 \cdot \tau_0 \le t < 1 \cdot \tau_0) = \overline{y}_0 = \frac{x(1 \cdot \tau_0) - x(0 \cdot \tau_0)}{\tau_0} = \frac{x_1 - x_0}{\tau_0}$$
$$\overline{y}(1 \cdot \tau_0 \le t < 2 \cdot \tau_0) = \overline{y}_1 = \frac{x(2 \cdot \tau_0) - x(1 \cdot \tau_0)}{\tau_0} = \frac{x_2 - x_1}{\tau_0}$$
$$\vdots$$
$$\overline{y}((N-2) \cdot \tau_0 \le t < (N-1) \cdot \tau_0) = \overline{y}_{M-1} = \frac{x((N-1) \cdot \tau_0) - x((N-2) \cdot \tau_0)}{\tau_0} = \frac{x_{N-1} - x_{N-2}}{\tau_0}$$
(1.11)

Here $M = N - 1$ is the number of fractional frequency data points. The time series obtained with the averaged fractional frequencies is represented by $\overline{y}(t) \equiv \{\overline{y}_0, \overline{y}_1, \overline{y}_2, \overline{y}_3, \overline{y}_4, ...\overline{y}_{M-1}\}$, and will provide the required data to characterize the stability associated with a particular pair of clocks. This is a very straightforward

procedure since the time deviations $x(m \cdot \tau_0)$ are just the differences in time between clocks, which can be measured with a counter and with negligible measurement noise (on the order of picoseconds).

If *M* values of averaged fractional frequency $\overline{y}_i$ are computed using (1.11), there are many ways to analyze these data. Historically, people have used the sample standard deviation as a measure of variability for the statistic $\overline{y}_i$ and estimated by:

$$\hat{\sigma}_{std.dev} = \sqrt{\frac{1}{M-1} \cdot \sum_{i=1}^{M} (\overline{y}_i - \overline{y})^2} \tag{1.12}$$

The usual convention of using the same symbol for the definition and for the estimator of quantities is followed in this thesis, except that estimators, as in expression (1.12), will be represented with a "hat" to avoid confusion. In the last expression, $\overline{y}$ represents the average fractional frequency over all the data set.

This approach presents several difficulties; in particular, depending on the spectral components present in the noise, the classical or sample standard deviation may not converge to a fixed value [11], (it only converges for White Noise Frequency Modulation WFM). In general, it is a function of the number of time data points *N*, which is not acceptable. For example, for two clocks that have slightly different stable frequencies of oscillation, the standard deviation of the fractional frequency fluctuation is a monotonically increasing function of the sample size and increases without limit (see Figure 2). It is clear that some other measure of variability of the fractional frequency must be chosen. The IEEE has adopted a standard measure known as the "Allan variance"[3] also known as two-sample variance.

Figure 2, obtained from [10], shows the ratio of the usual sample variance to the Allan variance as a function of the number of samples *N* for the five classes of noise present in clocks. It shows why the sample variance is not a convenient measure of

frequency stability; i.e. the number of samples in the computation has a very significant effect in the final value of the estimate, the lack of convergence is also evident except for the White Noise Frequency Modulation.

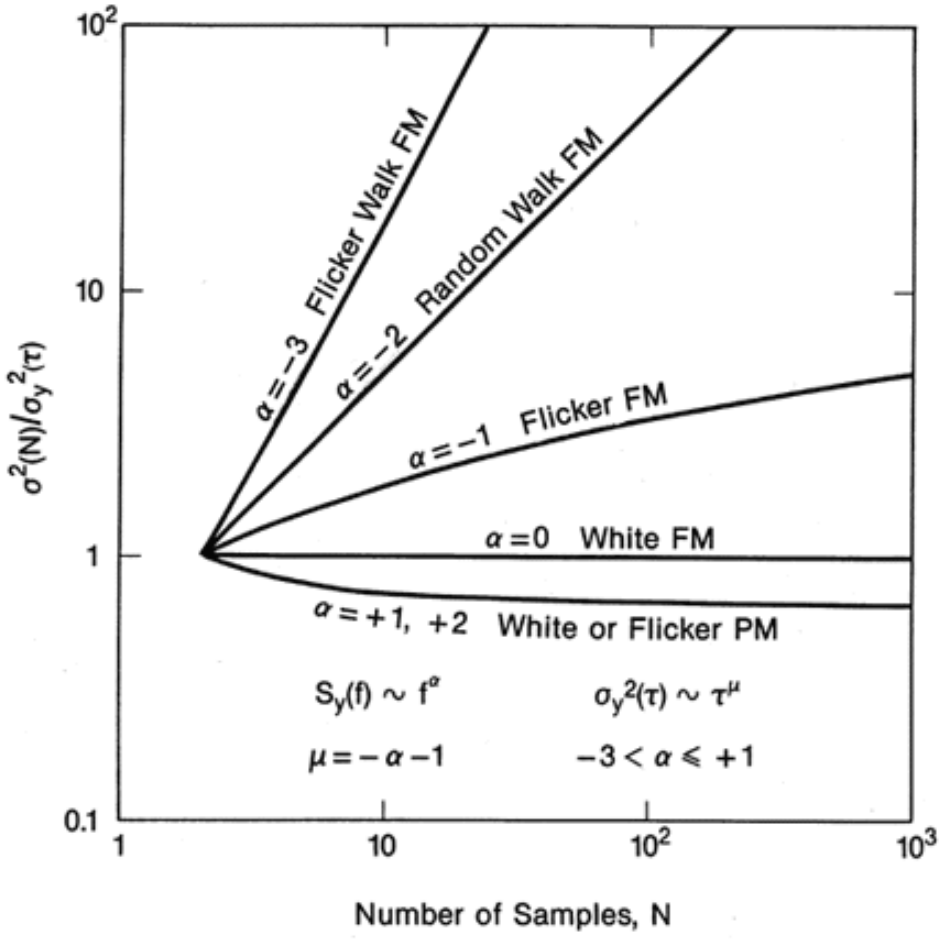

Figure 2. Ratio of sample /Allan variance for different noise processes (After ref. [10])

The square root of the Allan variance is called Allan deviation and is defined by:

$$\sigma_y(\tau) \equiv \left\langle \frac{1}{2} \cdot \left(\bar{y}(t+\tau) - \bar{y}(t)\right)^2 \right\rangle^{1/2}, \tau \geq 0 \qquad (1.13)$$

Where the symbols "$\langle\ \rangle$" denote infinite time average and the function $\bar{y}(t)$ is represented by the piecewise linear function obtained from the series

$\{\overline{y}_1, \overline{y}_2, \overline{y}_3, \overline{y}_4, ...\overline{y}_M\}$ computed at intervals of τ time units as in (1.11). The factor of ½ appearing in the definition (1.13) is introduced only for normalization purposes, when there are only two data samples, the classical standard deviation and the Allan deviation have exactly the same value as shown in Figure 2, no matter what kind of noise process is present. In practice, $\sigma_y(\tau_0)$ can be estimated from a finite set of *M* fractional frequency data points as follows:

$$\hat{\sigma}_y(\tau_0) = \sqrt{\frac{1}{2\cdot(M-1)}\sum_{i=1}^{M-1}\left(\overline{y}_{i+1} - \overline{y}_i\right)^2} \tag{1.14}$$

Again, the estimator has been represented with the "hat" notation. The relationship between the Allan deviation and the classical Standard deviation as a function of the sample size *N* for the common types of noise is shown in Table 2:

Noise Type	Standard deviation $\sigma_{std.dev}$
Random Walk Frequency Modulation	$\sigma_{std.dev} = \sigma_y(\tau)\cdot\sqrt{\frac{N}{2}}$
Flicker Frequency Modulation	$\sigma_{std.dev} = \sigma_y(\tau)\cdot\sqrt{\frac{N\cdot\log(N)}{2\cdot(N-1)\cdot\log(2)}}$
White Frequency Modulation	$\sigma_{std.dev} = \sigma_y(\tau)$
Flicker Phase Modulation	$\sigma_{std.dev} \approx \sigma_y(\tau)\cdot\sqrt{\frac{2\cdot(N-1)}{3\cdot N}}$
White Phase Modulation	$\sigma_{std.dev} = \sigma_y(\tau)\cdot\sqrt{\frac{2\cdot(N-1)}{3\cdot N}}$

Table 2. Relationship between classical standard deviation and Allan deviation (After ref. [18])

The same concept of Allan variance can be generalized to include Allan covariance between two time series. For two given time series of fractional frequencies

$\overline{y}^1(t)$ and $\overline{y}^2(t)$ defined according to (1.11), the Allan covariance of the two series is defined by:

$$\sigma_{y^1y^2}(\tau) \equiv \left\langle \frac{1}{2} \cdot \left(\overline{y}_1(t+\tau) - \overline{y}_1(t)\right) \cdot \left(\overline{y}_2(t+\tau) - \overline{y}_2(t)\right) \right\rangle, \tau \geq 0 \quad (1.15)$$

which can also be estimated by:

$$\hat{\sigma}_{y^1y^2}(\tau_0) = \frac{1}{2 \cdot (M-1)} \sum_{i=1}^{M-1} \left(\overline{y}_{i+1}^1 - \overline{y}_i^1\right) \cdot \left(\overline{y}_{i+1}^2 - \overline{y}_i^2\right) \quad (1.16)$$

There is an alternative definition of the Allan deviation and Allan covariance as a function of the time deviation series, $x(t)$, instead of the fractional frequency. For the Allan deviation it can be derived from (1.13) and (1.10):

$$\sigma_y(\tau) = \left\langle \frac{1}{2 \cdot \tau^2} \times \left(-x(t+2 \cdot \tau) + 2 \cdot x(t+\tau) - x(t)\right)^2 \right\rangle^{1/2}, \tau \geq 0 \quad (1.17)$$

The corresponding estimator is:

$$\hat{\sigma}_y(\tau_0) = \sqrt{\frac{1}{2 \cdot (N-2) \cdot \tau_0^2} \times \sum_{i=1}^{N-2} \left(-x_{i+2} + 2 \cdot x_{i+1} - x_i\right)^2} \quad (1.18)$$

Expressions (1.14) or (1.18) estimate the Allan variance for an integrating time equal to the sampling period τ_0, but values of the Allan variance for integrating times multiples of τ_0 are also needed because, as will be shown later, they allow us to estimate the type of noise process present in the data. The process for computing values of $\sigma_y^2(\tau = m \cdot \tau_0)$ at multiples *m* of the fundamental sampling period τ_0 is straightforward. Starting from the initial time series containing the fractional frequency values $\{\overline{y}_1, \overline{y}_2, \overline{y}_3, \overline{y}_4, ...\overline{y}_M\}$, to compute the Allan variance or deviation for an integrating time of $\tau = m \cdot \tau_0$ it is only required to obtain a new time series derived from the original where each term is an average of a subset of *m* terms of the original data set and is computed as [11]:

$$\overline{y}_i' = \frac{\overline{y}_{m \cdot i} + \overline{y}_{m \cdot i+1} + \overline{y}_{m \cdot i+2} + ... + \overline{y}_{m \cdot i+m-1}}{m} \quad (1.19)$$

Once the new time series $\{\overline{y}_0', \overline{y}_1', \overline{y}_2', \overline{y}_3', \overline{y}_4', ...\overline{y}_{M'-1}\}$ has been obtained, the expression given in (1.14) can be used to find $\hat{\sigma}_y(m\cdot\tau_0)$, in this case, M' represents the number of terms in the new series. This process can be done for any multiple of τ_0, but in practice, this computation is usually done for multiples that are powers of 2, i.e. $m = 1, 2, 4, 8, \ldots$.

Because of the averaging process involved in the computation of the new time series when $m \neq 1$, as the number m increases, there are less data points to compute $\sigma_y(m\cdot\tau_0)$ and consequently the confidence interval for $\sigma_y(m\cdot\tau_0)$ also increases. To minimize this negative effect, modern algorithms make a better use of the data available obtaining smaller confidence intervals. The standard algorithm used to compute the statistic is the overlapped algorithm and uses the time deviation series or raw data obtained from the clock comparison: $x_i, \forall i = \{0,1,2,...,N-1\}$, the overlapped estimate is given by [3]:

$$\hat{\sigma}_y(m\cdot\tau_0) = \sqrt{\frac{1}{2\cdot(N-2\cdot m)\cdot m^2\cdot\tau_0^2}\times\sum_{i=1}^{N-2\cdot m}\left(-x_{i+2\cdot m}+2\cdot x_{i+m}-x_i\right)^2} \quad (1.20)$$

The fact that the Allan variance or Allan deviation does converge for the five types of noise present in precision oscillators makes it suitable to measure the variability of the fractional frequency. However, it is not the only statistic that shows this property, other variances widely used with similar properties include The Modified Allan variance [12,13], The Total variance[11], The Time variance[14], The Hadamard variance (or three-sample variance)[15] and others [16,17].

The Allan variance also presents some inconveniences; the most important is that by using the Allan variance is not possible to differentiate White Phase Modulation (WPM) noise from Flicker Phase Modulation (FPM) noise. When those types of noise are present and a more accurate characterization is needed, then other statistics that are

capable of discriminating these two processes can be used, like the modified Allan variance [12].

2. A Simple Example to Compute Allan Variance.

To illustrate the computation of the Allan variance or Allan deviation, a simple example is provided below. Let us suppose that the time differences between two clocks have been measured every second and nine measurements have been made. The real time difference between them $x(t)$ is a continuous function represented in Figure 3, but only nine data samples are known.

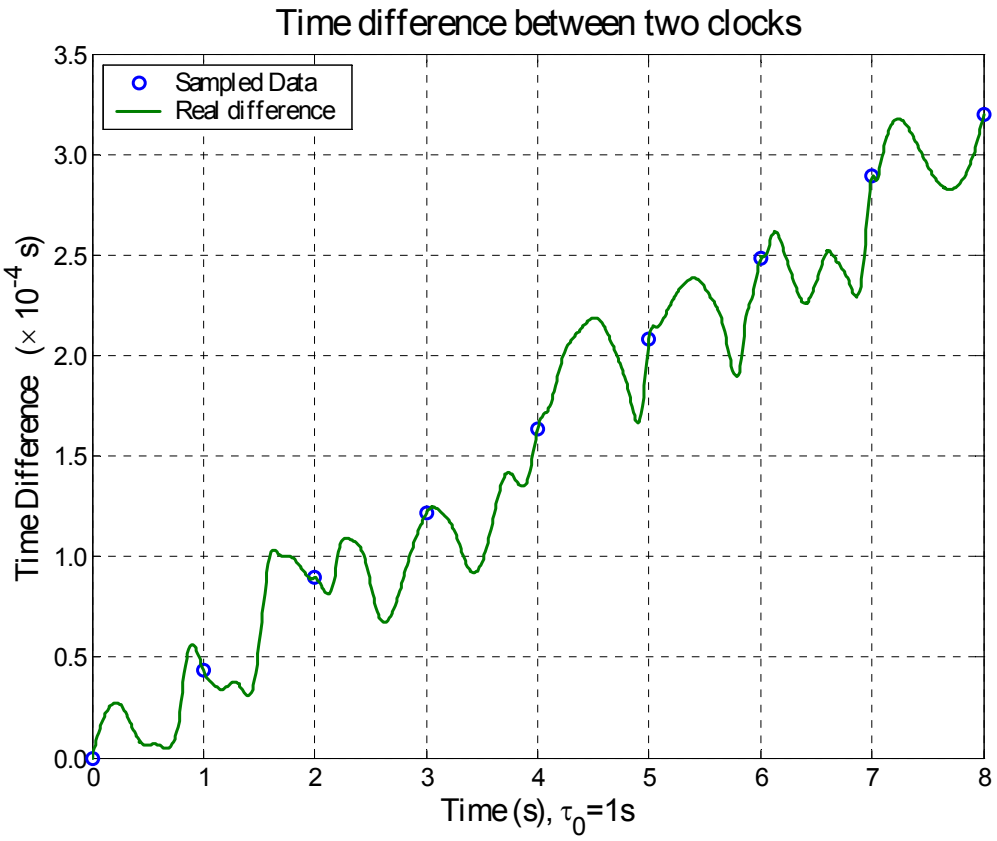

Figure 3. Sample data to compute Allan variance

The interval between samples is $\tau_0 = 1$ second, so the Allan variance can be computed at multiples of this τ_0: $\tau = n \cdot \tau_0, \quad n = \{1, 2, 3, ...\}$. The computation for $\tau = 1s$ is given in Table 3.

K	x_k $(\times 10^{-6})$	$\overline{y}_k = (x_{k+1} - x_k)/\tau$ $(\times 10^{-6})$	$\overline{y}_{k+1} - \overline{y}_k$ $(\times 10^{-6})$	$(\overline{y}_{k+1} - \overline{y}_k)^2$ $(\times 10^{-12})$	$\sigma_y(\tau = 1)$ $(\times 10^{-6})$
0	$x_0 = 0$	$\overline{y}_0 = 43.6$	2.5	6.25	
1	$x_1 = 43.6$	$\overline{y}_1 = 46.1$	-14.2	201.64	
2	$x_2 = 89.7$	$\overline{y}_2 = 31.9$	10.2	104.04	
3	$x_3 = 121.6$	$\overline{y}_3 = 42.1$	2.6	6.76	
4	$x_4 = 163.7$	$\overline{y}_4 = 44.7$	-5.1	26.01	5.67
5	$x_5 = 208.4$	$\overline{y}_5 = 39.6$	1.4	1.96	
6	$x_6 = 248.0$	$\overline{y}_6 = 41.0$	-10.2	104.04	
7	$x_7 = 289.0$	$\overline{y}_7 = 30.8$	----	----	
8	$x_8 = 319.8$	----	----	----	

Table 3. Steps for computing Allan deviation for $\tau = 1s$

Where $\sigma_y(\tau = 1)$ is computed as:

$$\sigma_y(\tau = 1) = \sqrt{\frac{1}{2 \cdot 7} \sum_{k=0}^{6} \left(\overline{y}_{k+1} - \overline{y}_k\right)^2} = 5.67 \cdot 10^{-6} s \qquad (1.21)$$

For values of τ different than τ_0, the computation follows a similar process. However, the classical estimate does not use all of the samples of time differences available. The steps to compute $\sigma_y(\tau = 2)$ is given in Table 4:

K	x_k $(\times 10^{-6})$	$\overline{y}_k = (x_{k+2} - x_k)/\tau$ $(\times 10^{-6})$	$\overline{y}_{k+2} - \overline{y}_k$ $(\times 10^{-6})$	$(\overline{y}_{k+2} - \overline{y}_k)^2$ $(\times 10^{-12})$	$\sigma_y(\tau = 2)$ $(\times 10^{-6})$
0	$x_0 = 0$	$\overline{y}_0 = 44.85$	-7.85	61.62	
1	$x_1 = 43.6$	----	----	----	
2	$x_2 = 89.7$	$\overline{y}_2 = 37.00$	5.15	26.52	
3	$x_3 = 121.6$	----	----	----	
4	$x_4 = 163.7$	$\overline{y}_4 = 42.15$	-6.25	39.06	4.60
5	$x_5 = 208.4$	----	----	----	
6	$x_6 = 248.0$	$\overline{y}_6 = 35.90$	----	----	
7	$x_7 = 289.0$	----	----	----	
8	$x_8 = 319.8$	----	----	----	

Table 4. Steps for computing Allan deviation for $\tau = 2s$

Where $\sigma_y(\tau = 2)$ is computed as:

$$\sigma_y(\tau = 2) = \sqrt{\frac{1}{2 \cdot 3} \sum_{k=0}^{2} \left(\overline{y}_{2k+2} - \overline{y}_{2k} \right)^2} = 4.60 \cdot 10^{-6} s \qquad (1.22)$$

A better algorithm to estimate the Allan variance for values of τ different than τ_0 should use all available fractional frequency data. This is what the overlapped estimate does. It is the algorithm used in this thesis. Both estimators are unbiased for the Allan variance, but in the case of the overlapped version, the confidence interval is smaller. Confidence intervals for the Allan variance will be treated in the next section. The overlapped algorithm to compute the Allan variance is shown in Table 5:

K	x_k $(\times 10^{-6})$	$\overline{y}_k = (x_{k+2} - x_k)/\tau$ $(\times 10^{-6})$	$\overline{y}_{k+2} - \overline{y}_k$ $(\times 10^{-6})$	$(\overline{y}_{k+2} - \overline{y}_k)^2$ $(\times 10^{-12})$	$\sigma_y(\tau = 2)$ $(\times 10^{-6})$
0	$x_0 = 0$	$\overline{y}_0 = 44.85$	-7.85	61.62	
1	$x_1 = 43.6$	$\overline{y}_1 = 39.00$	4.40	19.36	
2	$x_2 = 89.7$	$\overline{y}_2 = 37.00$	5.15	26.52	
3	$x_3 = 121.6$	$\overline{y}_3 = 43.40$	-3.10	9.61	
4	$x_4 = 163.7$	$\overline{y}_4 = 42.15$	-6.25	39.06	3.95
5	$x_5 = 208.4$	$\overline{y}_5 = 40.30$	----	----	
6	$x_6 = 248.0$	$\overline{y}_6 = 35.90$	----	----	
7	$x_7 = 289.0$	----	----	----	
8	$x_8 = 319.8$	----	----	----	

Table 5. Steps for computing (overlapped) Allan deviation for $\tau = 2s$

Where $\sigma_y(\tau = 2)$ is computed as:

$$\sigma_y(\tau = 2) = \sqrt{\frac{1}{2 \cdot 5} \sum_{k=0}^{4} \left(\overline{y}_{k+2} - \overline{y}_k\right)^2} = 3.95 \cdot 10^{-6} s \qquad (1.23)$$

3. Confidence Intervals for the Allan Variance.

The simplest method to compute the confidence intervals for $\sigma_y(\tau)$ [3,6,11], which assumes a symmetric Gaussian distribution, uses the following expression to compute 95% confidence intervals for the Allan variance [19]:

$$I_\alpha \cong 1.96 \cdot \sigma_y(\tau) \cdot \kappa_\alpha / \sqrt{N} \qquad (1.24)$$

where I_α is the half amplitude of the interval, κ_α is a constant related to the type of noise present and N is the number of data points used in the estimate and α corresponds to the slope in logarithm axes of $\log(PSD)$ vs. $\log(f)$.

The values for κ_α for the different noise types are given in Table 6.

Noise Type	RWFN	FFM	WFM	FFP	WPM
α	-2	-1	0	+1	+2
κ_α	0.75	0.75	0.87	0.99	0.99

Table 6. Values of κ_α to compute confidence intervals for σ_y^2

Another approach to computing confidence intervals is based on the distribution of the estimate for the Allan variance. The Allan variance estimator is distributed according to a Chi-Squared distribution[6,11]:

$$\chi^2 = \frac{d.f. \times s^2}{\sigma^2} \tag{1.25}$$

Where s^2 is the sample Allan variance, *d.f.* corresponds to the degrees of freedom and σ^2 is the true value of the Allan variance. The unknown parameter in the computation is the degrees of freedom of the distribution. Much research has been done in the past regarding the number of degrees of freedom. Both analytical and empirical expressions have been proposed[6]. The number of degrees of freedom depends on the algorithm used to compute the Allan variance and more importantly on the type of noise process present in the clocks. In this thesis, the algorithm used to compute the Allan variance is the overlapped version since it provides smaller confidence intervals for the same number of data points.

The empirical expressions for the number of degrees of freedom that are recommended in characterization of precision oscillators are given in Table 7 for the overlapped Allan variance.

Noise type	Degrees of Freedom
Random Walk Frequency Modulation (RWFM)	$\frac{N-2}{m}\times\frac{(N-1)^2-3\cdot m\cdot(N-1)+4\cdot m^2}{(N-3)^2}$
Flicker Frequency Modulation (FFM)	$\frac{2\cdot(N-2)^2}{2.3\cdot N-4.9}\quad(m=1)$ $\frac{5\cdot N^2}{4\cdot m\cdot(N+3\cdot m)}\quad(m\geq 2)$
White Frequency Modulation (WFM)	$\frac{4\cdot m^2}{4\cdot m^2+5}\times\left(\frac{3\cdot(N-1)}{2\cdot m}-\frac{2\cdot(N-2)}{N}\right)$
Flicker Phase Modulation (FPM)	$\sqrt{\exp\left(\log\left(\frac{N-1}{2\cdot m}\right)\times\log\left(\frac{(2\cdot m+1)\times(N-1)}{4}\right)\right)}$
White Phase Modulation (WPM)	$\frac{(N+1)\times(N-2\cdot m)}{2\cdot(N-m)}$

Table 7. Empirical expressions for the degrees of freedom of overlapped Allan variance (After ref. [3])

4. Time – Frequency Duality.

The characterization of precision clocks or oscillators can be done in both domains: time or frequency. The noise processes that may be present are defined in the frequency domain because this domain provides an adequate and straightforward definition by using the Power Spectral Density function. However, the duality between both domains permits us to identify the type of noise present while working exclusively in the time domain. That is, the plot of the Allan variance or Allan deviation for different values of τ almost completely characterizes the process [3] (for a complete characterization in the time domain the modified Allan variance could be used instead).

When the Allan variance is plotted on logarithm axes, the slope of the curve μ is related to the noise type according to Table 8 [3,6,10]:

Noise Process	Time Domain		
	σ_y^2	σ_y	Mod σ_y
Slope: $\log(\sigma_y(\tau))\ vs.\ \log(\tau)$ μ, μ'	μ	$\mu/2$	μ'
Random Walk Frequency Modulation	1	1/2	1/2
Flicker Frequency Modulation	0	0	0
White Frequency Modulation	-1	-1/2	-1/2
Flicker Phase Modulation	-2	-1	-1
White Phase Modulation	-2	-1	-1/2

Table 8. Noise processes used in modeling frequency instability (Time)

Complete characterization in the time domain is not possible using only the Allan variance. In Table 8, White Phase Modulation and Flicker Phase Modulation show the same slope. However, the modified Allan variance provides a way to separate them, as shown in the fourth column.

THIS PAGE INTENTIONALLY LEFT BLANK

II. CHARACTERIZATION OF THE CLOCK ENSEMBLE

A. STATEMENT OF THE PROBLEM

Each clock has its own intrinsic characteristics that have an immediate effect on the stability of the time scale that it generates. Unfortunately, it is not possible to perform absolute measurements on a particular clock because there is not a perfect clock to compare to. We can only measure the time phase difference between pairs of real clocks. In other words, we only have access to relative measurements that involve the instabilities generated inside both clocks.

The main effort in this chapter is to find an absolute measure of performance associated with each clock in order to assign a weight that will later be used to build an ensemble scale. The number of clocks belonging to the ensemble is represented by K. The available data to conduct this study is data obtained in laboratory consisting of K-1 time differences measured between all K clocks in the ensemble with respect to one arbitrary clock that is chosen as a reference. These time differences are measured at equally spaced instants of time and therefore each pair of clocks generates a time series.

Here is an important observation related to the concepts of stability and its change with time. In the rest of this thesis, the quantity "time" is simultaneously playing the role of both dependent and independent variable. The main objective of this work is devoted to characterization of the goodness of the time scale generated by each source of time or clock. The assumption that there is not a perfect time scale generator seems to contradict the idea that comparisons between real clocks are taken at "equally-spaced" instants of time. Obviously, there are not such "equally-spaced" instants of time since there is instability always present, but it is important to understand the different orders of magnitude that are related to "time" when it is playing the role of dependent or independent variable. Typical instabilities of atomic clocks are in the order of a few

nanoseconds per day, the nanoseconds measure the instability (dependent variable) while the day is the order of the independent variable and it makes no significant difference if the length of the day is 24 hours or 24 hours $\pm$ a few nanoseconds.

B. CONSTRUCTING A COMPOSITE CLOCK

One of the final goals in the characterization of the ensemble of clocks is the construction of an optimum time scale with respect to the stability in the frequency that it generates. In order to do that, the time varying behavior of each clock must be analyzed and an ensemble weight for each clock must be computed.

Let $\bar{\boldsymbol{y}} = \left(\bar{y}_1, \bar{y}_2, ..., \bar{y}_K\right)^T$ be a vector of averaged fractional frequencies corresponding to an averaging time τ for the K clocks belonging to the ensemble. Let $z = \boldsymbol{w} \cdot \bar{\boldsymbol{y}}$ be a scalar composite fractional frequency where $\boldsymbol{w}$ is the vector of weights given by $\boldsymbol{w} = \left(w_1, w_2, ..., w_K\right)$. If $\bar{\boldsymbol{y}}$ is multivariate normal with mean 0 and covariance matrix $\boldsymbol{R}$, what should the weights be in order to minimize the variance of z?

The traditional way to assign a weight to each clock is based on the variance terms of $\boldsymbol{R}$, that is, the elements in the main diagonal. Since $\boldsymbol{R}$ represents the covariance matrix of the fractional frequency deviations, the bigger the variance term corresponding to a particular clock, the more variability in the generated frequency and consequently, the less weight should be assigned to that clock.

The mathematical function used to assign weights generates them proportionally to the inverse of the corresponding variance term subjected to the condition that all of the weights must add up to 1. For example, for an ensemble of three clocks with covariance terms given by r_{11}, r_{22} and r_{33}, the corresponding weights are computed by:

$$
\begin{aligned}
w_1 &= \frac{1/r_{11}}{1/r_{11}+1/r_{22}+1/r_{33}} \\
w_2 &= \frac{1/r_{22}}{1/r_{11}+1/r_{22}+1/r_{33}} \\
w_3 &= \frac{1/r_{33}}{1/r_{11}+1/r_{22}+1/r_{33}}
\end{aligned}
\tag{2.1}
$$

In general, for an ensemble of K clocks, the weight of clock i can be obtained by:

$$
w_i = \frac{1/r_{ii}}{\sum_{j=1}^{K} 1/r_{jj}} \qquad \forall i \in \{1,2,...,K\} \tag{2.2}
$$

This classical approach is derived from the Three Cornered Hat method, in which the clocks are assumed to be uncorrelated and $\boldsymbol{R}$ is therefore diagonal.

When correlations between clocks occur, $\boldsymbol{R}$ is no longer diagonal and a more accurate technique can be used instead. If the weights of the clocks are grouped in the vector $\boldsymbol{w}$, the weights can be obtained in general by minimizing the variance of z subjected to the constraint that the weights must add up to 1 for the solution to be unbiased:

$$
\begin{aligned}
&\underset{w_i}{\text{Min}} \quad Var(z) = \boldsymbol{w}\cdot\boldsymbol{R}\cdot\boldsymbol{w}^T \\
&\text{s.t.} \qquad \boldsymbol{B}\cdot\boldsymbol{w}^T = 1
\end{aligned}
\tag{2.3}
$$

Here the vector $\boldsymbol{B}$ is a vector of K ones: $\boldsymbol{B} = (1,1,1,...,1)$.

Since $\boldsymbol{R}$ is symmetric and non-singular, it can be shown that there is only one stationary point for the function $\boldsymbol{w}\cdot\boldsymbol{R}\cdot\boldsymbol{w}^T$ subject to $\boldsymbol{B}\cdot\boldsymbol{w}^T = 1$ that is given by:

$$
\boldsymbol{w}^* = \boldsymbol{R}^{-1}\cdot\boldsymbol{B}^T\cdot\left(\boldsymbol{B}\cdot\boldsymbol{R}^{-1}\cdot\boldsymbol{B}^T\right)^{-1} \tag{2.4}
$$

This last equation can be used whenever $\boldsymbol{R}$ is no longer diagonal. When $\boldsymbol{R}$ is diagonal, both equations (2.2) and (2.4) provide the same results. Since the correlation between clocks is small in practice, there is little difference between the two approaches.

In any case, it is clear that knowledge of the matrix $\boldsymbol{R}$ is essential to the problem of constructing a composite time scale. We now turn to the problem of estimating $\boldsymbol{R}$.

C. MATHEMATICAL FORMULATION

Assume for the moment that there exists an ideal clock that provides a stable time scale and let x^i be a stochastic process associated with the i^{th} clock of the ensemble. Let now x_m^i be a realization of this process at the instance of time t_m. The interpretation of the stochastic processes x^i can be thought as the relative time deviation between the i^{th} clock and the ideal clock.

Let now the vector $\boldsymbol{x}^i = \left\{ x_k^i : k = 1, 2, ..., N \right\}$ be the sequence of N consecutive and equally spaced realizations of the process x^i. This vector contains the relative time deviation (differences) between clock i and an ideal clock measured at N different equally spaced instants of time.

$$\boldsymbol{x}^i = \left(x_1^i, x_2^i, x_3^i, ..., x_N^i \right)^T \tag{2.5}$$

The expected value of the process x^i can be estimated as a function of its elements as:

$$\overline{x}^i = \frac{1}{N}\left(x_1^i + x_2^i + ... + x_N^i \right) = \frac{1}{N}\sum_{k=1}^{N} x_k^i \tag{2.6}$$

and arranged into a constant vector of N elements as:

$$\overline{\boldsymbol{x}}^i = \left(\overline{x}^i, \overline{x}^i, \overline{x}^i, ..., \overline{x}^i \right)^T \tag{2.7}$$

For purposes of compactness, the expected values associated with all of the K processes for the clocks in the ensemble, can also be arranged in a $N \times K$ matrix:

$$\bar{\boldsymbol{X}} = \left(\bar{\boldsymbol{x}}^1, \bar{\boldsymbol{x}}^2, \bar{\boldsymbol{x}}^3, ..., \bar{\boldsymbol{x}}^K \right) \tag{2.8}$$

Likewise, the N samples or time differences between the K clocks and the ideal one can also be arranged into a similar $N \times K$ matrix:

$$\boldsymbol{X} = \left(\boldsymbol{x}^1, \boldsymbol{x}^2, \boldsymbol{x}^3, ..., \boldsymbol{x}^K \right) \tag{2.9}$$

If the K processes of time deviations are arranged in the vector $\boldsymbol{u}$ $\boldsymbol{u} = \left(x^1, x^2, x^3, ..., x^k \right)^T$, then the covariance matrix associated with the processes can be defined as:

$$\boldsymbol{R} = E\left\{ \boldsymbol{u} \cdot \boldsymbol{u}^T \right\} - E\left\{ \boldsymbol{u} \right\} \cdot E\left\{ \boldsymbol{u}^T \right\} \tag{2.10}$$

where the operator $E\{\ \}$ stands for mathematical expectation. Now, the covariance matrix of the processes associated with the available samples of time deviations for the K clocks in the ensemble can be estimated by [20,21,23]:

$$\hat{\boldsymbol{R}} = \frac{1}{N-1} \left(\boldsymbol{X} - \bar{\boldsymbol{X}} \right)^T \cdot \left(\boldsymbol{X} - \bar{\boldsymbol{X}} \right) \tag{2.11}$$

The $K \times K$ matrix $\boldsymbol{R}$ is referred to as the *absolute covariance matrix* since it is the covariance matrix involving the processes relating the time differences between real clocks in the ensemble with respect to fictitious ideal one. A generic element of the matrix $\boldsymbol{R}$ can be estimated by:

$$\hat{r}_{ij} = \frac{1}{N-1} \left(\boldsymbol{x}^i - \bar{\boldsymbol{x}}^i \right)^T \cdot \left(\boldsymbol{x}^j - \bar{\boldsymbol{x}}^j \right) \tag{2.12}$$

When $i = j$, $\hat{r}_{ij}$ represents the estimate of the variance of the time deviations of clock i and it is a nonnegative quantity; when $i \neq j$, $\hat{r}_{ij}$ represents the estimate of covariance between clocks i and j and can be positive or negative. The accuracy in the estimation of $\boldsymbol{R}$ improves with the number of samples available.

The final goal here is to estimate the *absolute covariance matrix* $\boldsymbol{R}$ in order to characterize the ensemble of clocks and to build a composite time scale using all of the clocks belonging to the ensemble. Unfortunately, there is no such ideal clock that has been assumed in the definition of the above quantities, consequently the elements r_{ij} of matrix $\boldsymbol{R}$ can not be directly computed or estimated because it is not possible to know the time differences x_k^i between the *j* clock and the ideal one at a particular time *k*.

Let us suppose that the ensemble of time standards consisting of *K* clocks of similar characteristics are arranged in such a way that it is possible to measure periodically the time differences of readings between each clock belonging to the ensemble and one arbitrary clock, also included in the ensemble, that has been chosen as a reference. Without loss of generality, let us assume that the K^{th} is chosen as the reference. At each particular instant of time, it is possible to measure all pairwise differences between the *K*-1 first clocks and the reference. In a strict sense, it is not possible to perform simultaneous measurements of all different pairs of clocks. However, since the time required to measure all pair-wise comparisons among all clocks is in the order of a few seconds and the time between successive measurements is in the order of days, the effect is always ignored (this can produce negative effects when not properly taken into account, as will be explained below).

It is then possible to express the measured data as a function of the differences of time between each clock and the ideal one, that is, let y_k^{ij} be the time difference of readings between clocks *i* and *j* at time *k*, then:

$$y_k^{ij} = x_k^i - x_k^j \tag{2.13}$$

At this point, a brief comment about notation is required. In Chapter I, the symbol "*y*" is used to represent fractional frequency. In this chapter, however, the same symbol is used along with sub and super indices to represent time differences between real clocks from an ensemble. There should be no confusion since the context in which this symbol

appears clearly identifies its meaning. Moreover, when the symbols y, $y(t)$, $\overline{y}$ or $\overline{y}_i$ are used, they always represent *fractional frequency deviation*. On the other hand, when superscripts are present as in y^{ij}, y_k^{ij}, $\overline{y}^i$ or $\overline{y}^{ij}$ they represent *time differences* between pairs of real clocks from the ensemble of clocks. To avoid confusion, the subscripts ***R*** or ***S*** will be always added to the "*y*" when representing fractional frequency deviation as in $\overline{y}_{\boldsymbol{R}k}^i$ or $\overline{y}_{\boldsymbol{S}k}^i$ respectively when referring to absolute or relative fractional frequency deviation.

Now, it is possible to think of y^{ij} as a different stochastic process that relates how the time differences between clocks *i* and *j* evolve with time. This process can be also characterized in terms of its expected value and variance. In particular, the variance of the process y^{ij} will be a function of the variances and covariance of the clocks *i* and *j* (r_{ii}, r_{jj} and r_{ij}). The goal here is to estimate the absolute quantities r_{ij} associated with each clock by using relative measurements among all pairs of clocks.

With an ensemble of *K* clocks it is possible, in theory, to obtain $K \cdot (K-1)/2$ processes, one per pair of different clocks. However, for real applications only *K*-1 of them are independent. The reason for this is that from the two sources of noise present in the model, the internal noise associated with each clock and the measurement noise, the last one is negligible. By only measuring the time differences between the first *K*-1 clocks and the K^{th} it is possible to find the differences between each other pair just by taking the difference of measurements with respect to the K^{th}.

When the K^{th} is chosen as a reference and the remaining *K*-1 clocks are compared to it at *N* different instants of time, the set of time-series measurements can be arranged in the following *N*-vectors: $\boldsymbol{y}^{1K} = \boldsymbol{x}^1 - \boldsymbol{x}^K$, $\boldsymbol{y}^{2K} = \boldsymbol{x}^2 - \boldsymbol{x}^K \ldots$ $\boldsymbol{y}^{K-1,K} = \boldsymbol{x}^{K-1} - \boldsymbol{x}^K$. And

finally, these K-1 processes containing the measurements can be arranged in the following $N \times (K-1)$ matrix:

$$\boldsymbol{Y} = \left(\boldsymbol{y}^{1K}, \boldsymbol{y}^{2K}, \boldsymbol{y}^{3K}, ..., \boldsymbol{y}^{K-1,K} \right) \tag{2.14}$$

The expected value of the processes y^{iK} can be estimated as a function of its elements as:

$$\overline{y}^{iK} = \frac{1}{N}\left(y_1^{iK} + y_2^{iK} + ... + y_N^{iK} \right) = \frac{1}{N}\sum_{k=1}^{N} y_k^{iK} \tag{2.15}$$

and arranged into a constant vector of N elements as:

$$\overline{\boldsymbol{y}}^{iK} = \left(\overline{y}^{iK}, \overline{y}^{iK}, \overline{y}^{iK}, ..., \overline{y}^{iK} \right)^T \tag{2.16}$$

Also, for purposes of compactness, the expected values associated with all of the processes for the clocks in the ensemble, can be arranged in the following $N \times (K-1)$ matrix:

$$\overline{\boldsymbol{Y}} = \left(\overline{\boldsymbol{y}}^{1K}, \overline{\boldsymbol{y}}^{2K}, \overline{\boldsymbol{y}}^{3K}, ..., \overline{\boldsymbol{y}}^{K-1,K} \right) \tag{2.17}$$

If the K–1 processes of relative time deviations y^{ik} are arranged in the vector $\boldsymbol{v}$ $\boldsymbol{v} = \left(y^{1k}, y^{2k}, y^{3k}, ..., y^{k-1,k} \right)^T$, then the covariance matrix associated with the processes can be defined as:

$$\boldsymbol{S} = E\left\{ \boldsymbol{v} \cdot \boldsymbol{v}^T \right\} - E\left\{ \boldsymbol{v} \right\} \cdot E\left\{ \boldsymbol{v}^T \right\} \tag{2.18}$$

Now, the covariance matrix of the processes associated with the available samples for the K-1 pair of clocks in the ensemble can be estimated by [20,21,23]:

$$\hat{\boldsymbol{S}} = \frac{1}{N-1}\left(\boldsymbol{Y} - \overline{\boldsymbol{Y}} \right)^T \cdot \left(\boldsymbol{Y} - \overline{\boldsymbol{Y}} \right) \tag{2.19}$$

The matrix $\boldsymbol{S}$ is referred to as the *relative covariance matrix* (in contrast with the *absolute covariance matrix* $\boldsymbol{R}$) since it is the covariance matrix involving the processes relating the time differences between real clocks in the ensemble with respect to another

real clock of the ensemble that is chosen as the reference. A generic element of the matrix $\boldsymbol{S}$ can be expressed as:

$$\hat{s}_{ij} = \frac{1}{N-1}\left(\boldsymbol{y}^{iK} - \overline{\boldsymbol{y}}^{iK}\right)^{T} \cdot \left(\boldsymbol{y}^{jK} - \overline{\boldsymbol{y}}^{jK}\right) \tag{2.20}$$

Each element of $\boldsymbol{S}$ represents a variance estimate if $(i = j)$ and is positive, or a covariance estimate if $(i \neq j)$ and can be positive or negative.

From now on, the superscript *K* will be omitted since the last clock will always be chosen as the reference.

D. CONSIDERATIONS ON THE COVARIANCE MATRICES *R* AND *S*

The absolute and relative covariance matrices $\boldsymbol{R}$ and $\boldsymbol{S}$ have been derived for the processes of time deviations obtained from comparative readings of clocks. However, the results for $\boldsymbol{R}$ and $\boldsymbol{S}$ are completely general for any other type of process. In particular, in frequency stability the processes that are commonly used are those obtained with fractional frequencies instead of time deviation. Since there is a linear relationship between time deviation and fractional frequencies (1.10) it is straightforward to convert from one to another and use fractional frequencies as the characteristic process. In this case, the matrices $\boldsymbol{R}$ and $\boldsymbol{S}$ represent a measure of variability of the internal frequency generated inside each clock. The less variability in the frequency corresponding to a particular clock the more stable it is and the higher its weight should be.

Our object is to find the absolute covariance matrix $\boldsymbol{R}$. Unfortunately, the elements of this matrix are not directly observable since the hypothetical perfect clock does not exist. On the other hand, the relative covariance matrix of fractional frequencies $\boldsymbol{S}$ can be estimated from relative measures between clocks from the ensemble. The next

section focuses on the relationship between these two matrices and the mathematical tools needed to obtain information about $\boldsymbol{R}$ starting from the estimation of $\boldsymbol{S}$.

1. Relationship Between the Matrices *R* and *S*.

The absolute and relative covariance matrices $\boldsymbol{R}$ and $\boldsymbol{S}$ are very closely related and can be estimated as functions of the time comparison of the K-1 pairs of clocks that form the ensemble. The dimension of the matrix $\boldsymbol{R}$ is $K \times K$ while the corresponding dimension for $\boldsymbol{S}$ is $(K-1)\times(K-1)$. Both are symmetric and positive semidefinite, consequently, there are $K \cdot (K+1)/2$ independent elements in $\boldsymbol{R}$ and $(K-1)\cdot K/2$ independent elements in $\boldsymbol{S}$. The matrix $\boldsymbol{S}$ can be estimated directly from the time measurements of the pairs of clocks, but the matrix $\boldsymbol{R}$ has K more elements than $\boldsymbol{S}$ so there is not a unique determination of $\boldsymbol{R}$ and an optimization criteria should be defined in order to find the "best" matrix $\boldsymbol{R}$.

The relationship between $\boldsymbol{R}$ and $\boldsymbol{S}$ can be derived by observing that the measurement matrices $\boldsymbol{X}$ and $\boldsymbol{Y}$ are related by:

$$\boldsymbol{Y} = \boldsymbol{X} \cdot \boldsymbol{H}\,, \tag{2.21}$$

where $\boldsymbol{H}$ is the $K \times (K-1)$ matrix:

$$\boldsymbol{H} = \begin{bmatrix} \boldsymbol{I} \\ -\boldsymbol{u}^T \end{bmatrix} \tag{2.22}$$

being $\boldsymbol{I}$ the $(K-1)\times(K-1)$ identity matrix and $\boldsymbol{u}^T$ the $(K-1)$ vector of ones:

$$\boldsymbol{u} = (1, 1, 1, ..., 1)^T \tag{2.23}$$

The matrices containing the expected values, $\overline{\boldsymbol{X}}$ and $\overline{\boldsymbol{Y}}$, are also equally related with matrix $\boldsymbol{H}$ as: $\overline{\boldsymbol{Y}} = \overline{\boldsymbol{X}} \cdot \boldsymbol{H}$

So that, finally, we have the following fundamental relationship between matrices $\boldsymbol{R}$ and $\boldsymbol{S}$:

$$\boldsymbol{S} = \boldsymbol{H}^T \cdot \boldsymbol{R} \cdot \boldsymbol{H} \tag{2.24}$$

For reasons that will become clear later, the covariance matrix $\boldsymbol{R}$ is partitioned separating the free and non-free parameters according to the following structure:

$$\boldsymbol{R} = \begin{pmatrix} \tilde{\boldsymbol{R}} & \boldsymbol{r}_{K-1} \\ \boldsymbol{r}_{K-1} & r_{KK} \end{pmatrix} \tag{2.25}$$

Here the matrix $\tilde{\boldsymbol{R}}$ is of order $(K-1)\times(K-1)$ and contains the first K-1 rows and columns of $\boldsymbol{R}$, and vector $\boldsymbol{r}_{K-1}$ is given by $\boldsymbol{r}_{K-1} \equiv \left(r_{1K}, r_{2K}, r_{3K}, ..., r_{K-1,K}\right)^T$. The relationship between $\boldsymbol{R}$ and $\boldsymbol{S}$ can be stated as:

$$\begin{aligned} \boldsymbol{S} = \boldsymbol{H}^T \cdot \boldsymbol{R} \cdot \boldsymbol{H} = \begin{bmatrix} \boldsymbol{I} & -\boldsymbol{u} \end{bmatrix} \times \begin{pmatrix} \tilde{\boldsymbol{R}} & \boldsymbol{r}_{K-1} \\ \boldsymbol{r}_{K-1} & r_{KK} \end{pmatrix} \times \begin{bmatrix} \boldsymbol{I} \\ -\boldsymbol{u}^T \end{bmatrix} = \\ \tilde{\boldsymbol{R}} + r_{KK} \cdot \begin{bmatrix} \boldsymbol{u} & \boldsymbol{u}^T \end{bmatrix} - \boldsymbol{u} \cdot \boldsymbol{r}_{K-1}{}^T - \boldsymbol{r}_{K-1} \cdot \boldsymbol{u}^T \end{aligned} \tag{2.26}$$

This last equation shows that $\boldsymbol{R}$ can be uniquely obtained from the matrix $\boldsymbol{S}$ once the elements contained in vector $\boldsymbol{r}_{K-1}$ and scalar r_{KK} are known.

During the process of estimation of clock instabilities, measurement data are usually pre-filtered to use for example, the Allan variance statistic instead of the classical variance/covariance. The derivation of matrices $\boldsymbol{R}$ and $\boldsymbol{S}$ is completely general and the relationship between them also holds when Allan variances and covariances are used inside $\boldsymbol{S}$ [21, 25]. This is the approach followed in this thesis and, unless otherwise stated, the variances and covariances used here will be the Allan (co)variances associated with the clock ensemble.

In order to obtain the matrix $\boldsymbol{S}$, the K^{th} clock of the ensemble is chosen as a reference and all of the pairwise comparisons among the other $K-1$ clocks and the K^{th} are used in the computation of $\boldsymbol{S}$.

2. A Simple Case with an Ensemble of *K*=3 clocks.

An example of an ensemble of three clocks is presented here for several reasons:

- It is possible to derive explicit expressions for the elements of $\boldsymbol{R}$ as functions of the corresponding elements of $\boldsymbol{S}$ and the problem is mathematically tractable [20].
- In the more general case when $K > 3$ the same approach will be followed but a final solution for matrix $\boldsymbol{R}$ will be obtained by numerically solving an optimization problem [21,22].
- There is an easy transition to the classical and widely used Three-Cornered Hat method [23].

If the number of clocks is three and the third is chosen as a reference, the available data are the N comparison samples between the pair of clocks 1 and 3 and between 2 and 3. The elements of the matrices $\boldsymbol{R}$, $\boldsymbol{S}$ and $\boldsymbol{H}$ are then:

$$\boldsymbol{R} = \begin{pmatrix} r_{11} & r_{12} & r_{13} \\ r_{12} & r_{22} & r_{23} \\ r_{13} & r_{23} & r_{33} \end{pmatrix} \tag{2.27}$$

$$\boldsymbol{S} = \begin{pmatrix} s_{11} & s_{12} \\ s_{12} & s_{22} \end{pmatrix} \tag{2.28}$$

$$\boldsymbol{H} = \begin{pmatrix} 1 & 0 \\ 0 & 1 \\ -1 & -1 \end{pmatrix} \tag{2.29}$$

And by using the relationship between them (2.24):

$$\boldsymbol{S} = \boldsymbol{H}^T \cdot \boldsymbol{R} \cdot \boldsymbol{H} \equiv \begin{pmatrix} s_{11} = r_{11} - 2 \cdot r_{13} + r_{33} & s_{12} = r_{12} - r_{13} - r_{23} + r_{33} \\ s_{12} = r_{12} - r_{13} - r_{23} + r_{33} & s_{22} = r_{22} - 2 \cdot r_{23} + r_{33} \end{pmatrix} \tag{2.30}$$

There are 3 equations in (2.30) corresponding to (s_{11}, s_{12}, s_{22}) that involve 6 unknown parameters: $(r_{11}, r_{12}, r_{13}, r_{22}, r_{23}, r_{33})$, consequently, there are infinitely many solutions to the problem of finding them. If the elements of $\boldsymbol{R}$ associated with the reference clock (r_{13}, r_{23}, r_{33}) are considered as free variables, then the remaining elements of $\boldsymbol{R}$ can be expressed as functions of them and the elements of $\boldsymbol{S}$ and the three equations become:

$$\begin{aligned} r_{11} &= s_{11} - r_{33} + 2 \cdot r_{13} \\ r_{12} &= s_{12} - r_{33} + r_{13} + r_{23} \\ r_{22} &= s_{22} - r_{33} + 2 \cdot r_{23} \end{aligned} \tag{2.31}$$

However, not all of the solutions are feasible. There are constraints to satisfy since the matrix $\boldsymbol{R}$ must be positive semidefinite. For a general matrix to be positive semidefinite it is necessary and sufficient that all the determinants of the principal minors of the matrix are positive. It could be thought that there are as many constraints as the number of principal minors in the matrix $\boldsymbol{R}$, that is, 3, but it is not the case here because the matrix $\boldsymbol{R}$ is not a general matrix. In [20,21] it is shown that since matrix $\boldsymbol{R}$ is obtained from matrix $\boldsymbol{S}$ which is already positive semidefinite, the only necessary and sufficient conditions for $\boldsymbol{R}$ to be positive semidefinite is that the determinant of $\boldsymbol{R}$ must be non-negative:

$$\left|\boldsymbol{R}\right| = r_{11} \cdot r_{22} \cdot r_{33} + 2 \cdot r_{12} \cdot r_{23} \cdot r_{13} - r_{13}^2 \cdot r_{22} - r_{12}^2 \cdot r_{33} - r_{23}^2 \cdot r_{11} \geq 0 \tag{2.32}$$

This means that there are now 3 equations (2.31), 1 constraint (2.32) and 6 unknowns . There are still infinitely many solutions.

3. Selection of the Free (Co)variances r_{13}, r_{23} and r_{33}.

An optimality criterion must be defined to reach a solution for the elements of the covariance matrix $\boldsymbol{R}$. The objective function proposed by [20] includes a global measure of covariance of the ensemble: quadratic mean covariance $G(\boldsymbol{R}) = \sqrt{\left(r_{12}^2 + r_{13}^2 + r_{23}^2\right)/3}$,

which can be expressed as a function of the free parameters grouped as $\boldsymbol{r}_3 = \left(r_{13}, r_{23}, r_{23}\right)^T$, and the elements of the relative covariance matrix $\boldsymbol{S}$ by using (2.30):

$$\begin{aligned}
&\left[G(\boldsymbol{R})\right]^2 = \left(r_{12}^2 + r_{13}^2 + r_{23}^2\right)/3 = \\
&\left[G(\boldsymbol{r}_3; \boldsymbol{S})\right]^2 = \\
&\qquad \big(\ 2\cdot\left(r_{13} - r_{33}\right)^2 + 2\cdot\left(r_{13} - r_{33}\right)\cdot\left(r_{23} - r_{33}\right) + \ldots \\
&\qquad 2\cdot\left(r_{23} - r_{33}\right)^2 + 2\cdot\left(2\cdot r_{33} + s_{12}\right)\cdot\left(r_{13} - r_{33}\right) + \ldots \\
&\qquad 2\cdot\left(2\cdot r_{33} + s_{12}\right)\cdot\left(r_{23} - r_{33}\right) + 2\cdot r_{33}^2 + \left(s_{12} + r_{33}\right)^2 \ \big)/3
\end{aligned} \tag{2.33}$$

Equation (2.33) can be generalized to any number of clocks by applying the basic linear relationship $\boldsymbol{S} = \boldsymbol{H}^T \cdot \boldsymbol{R} \cdot \boldsymbol{H}$ in order to express $G(\boldsymbol{R})$ as a function of the free parameters $\boldsymbol{r}_K$ and the elements of $\boldsymbol{S}$: $\left[G(\boldsymbol{r}_K; \boldsymbol{S})\right]^2$. It will be used as a component of two different objective functions that will be analyzed below. A. Premoli and P. Tavella [20] suggest an unconstrained optimization problem to find r_{13}, r_{23} and r_{33}. They minimize by choice of r_{13}, r_{23} and r_{33} the following objective function:

$$F(\boldsymbol{r}_3; \boldsymbol{S}) = \frac{3\cdot\sqrt{|\boldsymbol{S}|}\left[G(\boldsymbol{r}_3; \boldsymbol{S})\right]^2}{|\boldsymbol{R}|} \tag{2.34}$$

The idea is to minimize the "global correlation" among clocks while maintaining the positive semidefiniteness of $\boldsymbol{R}$. The combination of $G(\boldsymbol{r}_3; \boldsymbol{S})$ in the numerator and $|\boldsymbol{R}|$ in the denominator finds the matrix $\boldsymbol{R}$ with smallest global correlation and at the same time ensures the positive semidefiniteness of $\boldsymbol{R}$ by the presence of $|\boldsymbol{R}|$. If during the minimization process the incumbent solution approaches the boundary of the feasible region $|\boldsymbol{R}| = 0$, then the objective function's value increases showing that this is not a valid direction to minimize.

For the case of 3 clocks A. Premoli and P. Tavella showed that the solution to the minimization problem is unique and can be performed analytically to find the optimal values r_{13}^*, r_{23}^* and r_{33}^*.

4. The Classical Three-Cornered Hat Method.

The classical method most widely used to find the variances associated with each clock: r_{11}, r_{22} and r_{33} can be derived as a particular case of the method proposed above. The three-cornered hat method [20,26] assumes that the clocks are completely independent and uncorrelated. It means that, for the same case of three clocks, $r_{12} = r_{13} = r_{23} = 0$. Under this hypothesis, since the covariance matrices $\boldsymbol{R}$ and $\boldsymbol{S}$ are related by $\boldsymbol{S} = \boldsymbol{H}^T \cdot \boldsymbol{R} \cdot \boldsymbol{H}$, equation (2.30) becomes:

$$\boldsymbol{S} = \begin{pmatrix} s_{11} = r_{11} + r_{33} & s_{12} = r_{33} \\ s_{12} = r_{33} & s_{22} = r_{22} + r_{33} \end{pmatrix} \tag{2.35}$$

In order for $\boldsymbol{R}$ to be positive semidefinite, since $r_{11}, r_{22}, r_{33} \geq 0$ and also $s_{11}, s_{22} \geq 0$, the following conditions must be met:

$$s_{12} \geq 0, \quad s_{12} \leq s_{11}, \quad s_{12} \leq s_{22} \tag{2.36}$$

In that case, the solutions for r_{11}, r_{22} and r_{33} are the same that the ones obtained in the minimization problem and have a simple representation obtained from (2.31):

$$\begin{aligned} r_{11} &= s_{11} - s_{12} \\ r_{22} &= s_{22} - s_{12} \\ r_{33} &= s_{12} \end{aligned} \tag{2.37}$$

Since the solution involves a system of three simultaneous equations with three unknowns; there is no need to perform a minimization since there are no free parameters , and the condition of positive definiteness is consequently not imposed. As a consequence, the solution sometimes may produce negative values for the variances, which is not acceptable.

Several approaches to avoid the appearance of negative variances have been proposed, such as considering only the absolute value [27] or substituting its value by zero when negative results are obtained. None of them is based on theoretical or physical

considerations. They are just a means to avoid this nuisance. The causes leading to the estimation of negative variances when the popular three-cornered hat method is used are:

- Uncertainty in the measured time differences.
- Lack of contemporaneity of measurements.
- Presence of correlation between clocks.

When some of the above conditions are not met, the three-cornered hat method is no longer applicable. The introduction of free parameters requires the definition of a suitable minimization criterion in order to provide the analytical conditions to obtain the desired values for the free parameters. The optimality criterion is usually based on the minimization of some function that measures a global covariance associated with the whole ensemble of clocks.

5. Optimal Selection of the Free Covariances: Constrained or Unconstrained Minimization?

When the number of clocks in the ensemble is greater than three, it is shown in section **C.1** that the problem of finding the covariance matrix $\boldsymbol{R}$ from the covariance matrix of observations $\boldsymbol{S}$ is under determined. In particular, if the number of clocks in the ensemble is K, there are $K\cdot(K+1)/2$ independent elements in $\boldsymbol{R}$ and $K\cdot(K-1)/2$ independent elements in $\boldsymbol{S}$; therefore there are always exactly K free parameters to determine by means of a minimization problem. Unless otherwise stated, in the rest of this paper the election of the free parameters will be (co)variances associated with the clock that is chosen as the reference (which is also usually chosen as the one that is believed to have the best stability characteristics), i.e. the K^{th} clock in the ensemble. Then $r_{1K}, r_{2K}, r_{3K}, ..., r_{KK}$ constitute the decision variables of the problem. For compactness, group these in the vector $\boldsymbol{r}_K \equiv (r_{1K}, r_{2K}, r_{3K}, ..., r_{KK})^T$. The rest of the elements of the matrix

$\boldsymbol{R}$, that is, the ones that do not involve the K^{th} clock can be always expressed as functions of the elements of $\boldsymbol{S}$ and the decision variables:

$$r_{ij} = f_{ij}\left(\boldsymbol{r}_K; \boldsymbol{S}\right) \quad \forall i, j \in \{1, 2, 3, ..., K-1\} \tag{2.38}$$

The approaches followed in [21] and [25] suggest solving an unconstrained minimization problem with an objective function taking one of the following forms:

$$\begin{aligned} F_1\left(\boldsymbol{r}_K; \boldsymbol{S}\right) &= \frac{\left[G\left(\boldsymbol{r}_K; \boldsymbol{S}\right)\right]^2}{\left|R\left(\boldsymbol{r}_K; \boldsymbol{S}\right)\right|} \\ F_2\left(\boldsymbol{r}_K; \boldsymbol{S}\right) &= \frac{\left[G\left(\boldsymbol{r}_K; \boldsymbol{S}\right)\right]^2}{\left|R\left(\boldsymbol{r}_K; \boldsymbol{S}\right)\right|^2} \end{aligned} \tag{2.39}$$

where

$$\left[G\left(\boldsymbol{r}_K; \boldsymbol{S}\right)\right]^2 = \sum_{j=1}^{K} \sum_{i<j}^{K} r_{ij}^2 \tag{2.40}$$

The presence of the square of the determinant of $\boldsymbol{R}$ in the denominator provides, according to Torcasso [25], a better numerical convergence and helps to maintain the incumbent solution inside the feasible region given by $\left|R\left(\boldsymbol{r}_K; \boldsymbol{S}\right)\right| \geq 0$, In [21] it is shown that this expression has a nice closed form expression suitable for numerical computations:

$$\begin{aligned} &\left|\boldsymbol{R}\left(\boldsymbol{r}_K; \boldsymbol{S}\right)\right| = \\ &\left|\boldsymbol{S}\left(s_{ij}\right)\right| \cdot \left[\left(r_{KK} - \left[\boldsymbol{r}_{K-1} - r_{KK} \cdot \boldsymbol{u}\right]^T\right) \times \boldsymbol{S}^{-1} \times \left(r_{KK} - \left[\boldsymbol{r}_{K-1} - r_{KK} \cdot \boldsymbol{u}\right]\right)\right] \end{aligned} \tag{2.41}$$

6. New Proposal for the Constrained Minimization Problem.

The solution adopted in this paper is based on a generalization of the solution proposed in [22,24] which has an immediate physical interpretation. As a side effect, it can be used on clocks in an ensemble consisting of clocks from different laboratories.

The objective function based on the quadratic mean covariance $\left[G\left(\boldsymbol{r}_K;\boldsymbol{S}\right)\right]^2=\sum_{i=1}^{K}\sum_{i<j}^{K}r_{ij}^2$ has the attractive property of convexity in the space of the free parameters $\boldsymbol{r}_K$. However, the (co)variance terms are not normalized; they can take any value and can oscillate orders of magnitude from clock to clock – especially if the clocks do not have the same characteristics. The final solution can be greatly influenced by the characteristics of one particular clock. If the objective function is modified to be a "quadratic mean correlation" of the ensemble, instead of covariance, then the effect of one clock presenting big variance and covariance terms does not have such a big impact in the final solution obtained by the minimization. This effect will be shown with an example. This new objective function, the one that will be minimized in this thesis, has the following expression:

$$F_3\left(\boldsymbol{r}_K;\boldsymbol{S}\right)=\sum_{j=1}^{K}\sum_{i<j}^{K}\frac{r_{ij}^2}{r_{ii}\cdot r_{jj}} \tag{2.42}$$

In the approach presented here, one new set of constraints has been added to the minimization problem. To the knowledge of the author, no reports accounting for negative correlations between pairs of clocks under similar environmental conditions have been reported, so it makes sense to constrain the covariances or correlation coefficients to only non-negative values. Therefore, clocks from the same laboratory will be constrained to present positive correlations between them. Correlation between laboratories is unrestricted and consequently can take both positive or negative values. Negative correlations between laboratories could be caused by diurnal, seasonal or geographical factors.

7. Mathematical Formulation of the Minimization Problem.

The general minimization problem to be solved when two different laboratories are involved is:

$$\begin{aligned} \underset{\boldsymbol{r}_K}{\text{Min}} \quad & F_3\left(\boldsymbol{r}_K;\boldsymbol{S}\right)=\sum_{j=1}^{K}\sum_{i<j}^{K}\frac{r_{ij}^2}{r_{ii}\cdot r_{jj}} \\ \text{s.t.} \quad & \left|\boldsymbol{R}\left(\boldsymbol{r}_K;\boldsymbol{S}\right)\right|\geq 0 \\ & r_{ij}\left(\boldsymbol{r}_K;\boldsymbol{S}\right)\geq 0 \qquad \forall\, i,j\in C_1, i<j \\ & r_{ij}\left(\boldsymbol{r}_K;\boldsymbol{S}\right)\geq 0 \qquad \forall\, i,j\in C_2, i<j \end{aligned} \tag{2.43}$$

Where C_1 contains the indices of all clocks belonging to laboratory 1 and C_2 contains the indices of all clocks belonging to laboratory 2. The requirement of positive correlation among the clocks in the ensemble is assured by the constraints $r_{ij}(\boldsymbol{r}_K;\boldsymbol{S})\geq 0$.

For the simple case of an ensemble of *K* clocks, all from the same laboratory, the absolute covariance matrix $\boldsymbol{R}_{K\times K}$ consists of $\frac{K\cdot(K+1)}{2}$ different elements $r_{ij},\ \ i,j\in\{1,2,...,K\}$ that need to be determined. The relative covariance matrix $\boldsymbol{S}_{(K-1)\times(K-1)}$ has $\frac{K\cdot(K-1)}{2}$ different elements that are known from measured data. The relationship (2.24) among $\boldsymbol{R}$ and $\boldsymbol{H}$ then provides $\frac{K\cdot(K-1)}{2}$ distinct linear equations that relate the elements r_{ij} and s_{ij}, so there are only $\frac{K\cdot(K+1)}{2}-\frac{K\cdot(K-1)}{2}=K$ free parameters among the elements of $\boldsymbol{R}$. They are the decision variables and will be chosen as the elements of $\boldsymbol{R}$ associated with the K^{th} clock: $\boldsymbol{r}_K$. Before carrying out the minimization problem it is necessary to express the objective function and the constraints as functions of only the decision variables $\boldsymbol{r}_K$. Then, once the minimization problem has been solved, the remaining elements of $\boldsymbol{R}$ can be uniquely computed using again the linear equations that relate the matrices $\boldsymbol{R}$, $\boldsymbol{H}$ and $\boldsymbol{S}$.

E. ESTIMATION OF THE COVARIANCE MATRICES *R* AND *S*

1. Notation and Definitions.

Let the quantity x_m^i be a realization of the process x^i that represents the time difference between clock *i* and an ideal clock at the instant of time $m\tau_0$, where τ_0 is the sampling interval. Similarly, let y_m^i be a realization of the process y^i that represents the time difference between clock *i* and the K^{th} clock or reference at the instance of time $m\tau_0$. According to these conventions, the absolute and relative fractional frequencies can be expressed using (1.11) and the new notation as:

$$\overline{y}_{\boldsymbol{R}k}^i = \overline{y}_{\boldsymbol{R}k}^i(\tau_0) = \frac{x_{k+1}^i - x_k^i}{\tau_0} \tag{2.44}$$

And

$$\overline{y}_{\boldsymbol{S}k}^i = \overline{y}_{\boldsymbol{S}k}^i(\tau_0) = \frac{y_{k+1}^i - y_k^i}{\tau_0} \tag{2.45}$$

For $k \geq 1$, for intervals of time multiples of τ_0, the usual average of the fractional frequency (1.19) is always used:

$$\overline{y}_{\boldsymbol{S}k}^i(\tau = m \cdot \tau_0) = \frac{1}{m}\sum_{l=1}^{m} \overline{y}_{\boldsymbol{S}(k-1)m+l}^i \tag{2.46}$$

$$\overline{y}_{\boldsymbol{R}k}^i(\tau = m \cdot \tau_0) = \frac{1}{m}\sum_{l=1}^{m} \overline{y}_{\boldsymbol{R}(k-1)m+l}^i \tag{2.47}$$

Recall that both x^i and y^i represent the differences between clock *i* and an ideal clock and between clock *i* and clock *K*. Consequently, $\overline{y}_{\boldsymbol{R}k}^i$ and $\overline{y}_{\boldsymbol{S}k}^i$ represent average variations. If clock *i* is perfect then, $\overline{y}_{\boldsymbol{R}k}^i$ will be zero, but $\overline{y}_{\boldsymbol{S}k}^i$ does not have to be zero since clock *K* may not be perfect. If clock *i* is not perfect then $\overline{y}_{\boldsymbol{R}k}^i$ will characterize clock *i*, but $\overline{y}_{\boldsymbol{S}k}^i$ will include the instabilities associated with both clocks *i* and *K*. For each of

the first *K*-1 clocks in the ensemble, $\overline{y}^i_{\boldsymbol{S}k}$ represents a time series that will be used to estimate $\overline{y}^i_{\boldsymbol{R}k}$.

2. Estimation of Allan (Co)variances from the Measured Data.

The fractional frequency deviation time series associated with the *K*-1 pairs of clocks could be directly used to compute the $(K-1)\times(K-1)$ covariance matrix $\boldsymbol{S}$ using the raw data. However, this approach is never used in practice since there may be present different types of noise for which the usual variance does not converge as previously shown in Figure 2. Instead, the raw data are filtered in the time domain to obtain the covariance matrix $\boldsymbol{S}$ based on the Allan covariances instead of the traditional (co)variances.

Using the previous notation, the Allan variance associated with clock *i* referenced to clock *K* can be expressed using (1.13) as:

$$s_{ii}(\tau) = \frac{1}{2}\left\langle \left(\overline{y}^i_{\boldsymbol{S}k+1}(\tau) - \overline{y}^i_{\boldsymbol{S}k}(\tau)\right)^2 \right\rangle \tag{2.48}$$

and the Allan variance associated with clock *i* referenced to the ideal clock can be expressed as:

$$r_{ii}(\tau) = \frac{1}{2}\left\langle \left(\overline{y}^i_{\boldsymbol{R}k+1}(\tau) - \overline{y}^i_{\boldsymbol{R}k}(\tau)\right)^2 \right\rangle \tag{2.49}$$

where again, the $\langle\ \rangle$ denotes mathematical expectation or infinite time average. We assume that the process of averaged fractional frequencies is stationary and ergodic so that the last equation is well-defined.

Similarly, when $(i \neq j)$ the Allan covariances of clocks *i* and *j* referenced to clock *K* or referred to the ideal clock also can be written ,respectively, according to (1.15) as:

$$s_{ij}(\tau) = \frac{1}{2}\left\langle \left(\overline{y}^{i}_{\boldsymbol{S}k+1}(\tau) - \overline{y}^{i}_{\boldsymbol{S}k}(\tau)\right)\cdot\left(\overline{y}^{j}_{\boldsymbol{S}k+1}(\tau) - \overline{y}^{j}_{\boldsymbol{S}k}(\tau)\right)\right\rangle \tag{2.50}$$

$$r_{ij}(\tau) = \frac{1}{2}\left\langle \left(\overline{y}^{i}_{\boldsymbol{R}k+1}(\tau) - \overline{y}^{i}_{\boldsymbol{R}k}(\tau)\right)\cdot\left(\overline{y}^{j}_{\boldsymbol{R}k+1}(\tau) - \overline{y}^{j}_{\boldsymbol{R}k}(\tau)\right)\right\rangle \tag{2.51}$$

As usual, the covariance reduces to variance when $(i = j)$.

The covariance matrix $\boldsymbol{S}$ can now be directly estimated from the filtered data obtained from the time comparisons of the *K* clocks. The overlapped estimator given by [3] for a given $\tau = m \cdot \tau_0$ is:

$$\hat{s}_{ij}(\tau = m\cdot\tau_0) = \frac{1}{2(N-2m)}\times \sum_{k=1}^{N-2m}\left(\overline{y}^{i}_{\boldsymbol{S}k+1}(m\cdot\tau_0) - \overline{y}^{i}_{\boldsymbol{S}k}(m\cdot\tau_0)\right)\cdot\left(\overline{y}^{j}_{\boldsymbol{S}k+1}(m\cdot\tau_0) - \overline{y}^{j}_{\boldsymbol{S}k}(m\cdot\tau_0)\right) \tag{2.52}$$

and similarly for the elements of the covariance matrix $\boldsymbol{R}$:

$$\hat{r}_{ij}(\tau = m\cdot\tau_0) = \frac{1}{2(N-2m)}\times \sum_{k=1}^{N-2m}\left(\overline{y}^{i}_{\boldsymbol{R}k+1}(m\cdot\tau_0) - \overline{y}^{i}_{\boldsymbol{R}k}(m\cdot\tau_0)\right)\cdot\left(\overline{y}^{j}_{\boldsymbol{R}k+1}(m\cdot\tau_0) - \overline{y}^{j}_{\boldsymbol{R}k}(m\cdot\tau_0)\right) \tag{2.53}$$

The elements of the matrix $\boldsymbol{S}$ are computed from the time deviation series using equations (2.52), (2.46) and (2.45).

III. COMPARISON, TESTING AND SIMULATION

A. OVERVIEW

1. Description of the Different Tests Performed

The theoretical formulation of the method to compute the variability of the fractional frequency deviation associated with each particular clock in the ensemble has been stated in the last chapter. The next step in the analysis of the validity of the method involves some comparisons with results taken from other researchers, and also with simulations to test the accuracy and the response to dynamic changes in the parameters of the clocks.

Four different tests, increasing in complexity, are summarized below:

- A point comparison of the method for one particular artificial case analyzed by several authors. Comparable results with what others have obtained will give some insight about the possibilities of the new method.
- A simulation involving the generation of random covariance matrices as the starting point and use the 5 different methods described below in section III B, to solve the same problem. Three different *MOP*'s will be defined and used to compare the results provided by each approach.
- A simulation to test the dynamic behavior of the proposed method. Instead of generating random absolute covariance matrices $\boldsymbol{R}$, the variance terms associated with each clock will be changed according to a predefined function to test the sensitivity against small changes in the input data.
- The last simulation involves the solution of a complete problem. The phase or time data of each clock is generated including additive noise with predefined spectral characteristics and Allan variances. This simulation

involves the computation of the relative covariance matrix $\boldsymbol{S}$ from phase data, the minimization problem to derive the absolute covariance matrix $\boldsymbol{R}$ and the weights of each clock.

2. Analysis of the Uniform Random Number Generator.

Before entering into the specific details of the simulation it is worth saying that the software package used is *matlab*© (version 6.5) with the optimization toolbox (version 2.2). Extensive use of the Uniform Random Number Generator (URNG) built into *matlab* is required. Unfortunately, there is no information available about this particular URNG and so, before using it, the tests included in the diehard suite of tests created by Marsaglia [28] are applied to a 24MB file containing uniform random numbers generated in *matlab*. The steps to test the generator are summarized below:

- Generate 32-bit unsigned integers by mapping the range of the interval of the URNG $[0,1]$ into the integer interval $[0, 2^{32}-1]$ as required by the test specifications [28].
- Conversion of the 32-bit integers into 8-character hexadecimal numbers.
- Create a 24MB text file consisting of 80 character lines (10 numbers) with the numbers previously generated.
- Create a binary file using the last data file as input
- Finally, execute the test program and provide the binary file as input.

The results indicated that the URNG is of sufficient quality to proceed

3. Definition of Proposed Measures of Performance (*MOP*).

In order to test and compare the results derived in the simulation, three measures of performance are defined. They are based on the absolute covariance matrix, $\boldsymbol{R}$, and its

correlation matrix, $\boldsymbol{\rho}$. Just by looking at Table 9, is difficult to say which of them provide results closer to the true values of $\boldsymbol{R}$ and $\boldsymbol{\rho}$. In order to compare them, three different measures of performance (*MOP*) are defined:

MOP_1: Sum of the squared residuals of the elements of the computed $\boldsymbol{R}$.

$$MOP_1 = \sum_{j=1}^{K} \sum_{i \le j}^{K} \left(r_{ij} - \hat{r}_{ij} \right)^2 \tag{3.1}$$

MOP_2: Sum of the squared residuals of the elements of the correlation matrix $\boldsymbol{\rho}$.

$$MOP_2 = \sum_{j=1}^{K} \sum_{i \le j}^{K} \left(\rho_{ij} - \hat{\rho}_{ij} \right)^2 \tag{3.2}$$

MOP_3: Sum of the squared residuals of the elements corresponding to the variances of $\boldsymbol{R}$, that is, the diagonal terms of $\boldsymbol{R}$.

$$MOP_3 = \sum_{i=1}^{N} \left(r_{ii} - \hat{r}_{ii} \right)^2 \tag{3.3}$$

The third *MOP* is the simplest and the preferred one; the most important values in the matrix $\boldsymbol{R}$ are the variance terms located in the main diagonal, since they are directly used to compute the weighting factors for each clock.

B. TEST N°1, SINGLE POINT COMPARISON

In order to compare the approach presented here with previous approaches, the same sample matrix $\boldsymbol{S}$ that has been used by other authors [22,24], is used below so that the final solutions can be easily compared. The five methods used in the analysis are listed below:

- 1. Three-cornered hat method [20]
- 2. Tavella method [20]

- 3. Torcasso et al. method [25]
- 4. Galindo F. J. et al. method [22,24]
- 5. Proposed Ruiz-Galindo method.

The starting (simulated) covariance matrix $\boldsymbol{R}$ is based on an ensemble of four clocks having different characteristics and also includes correlation between different pairs of clocks. The covariance matrix $\boldsymbol{R}$ for this example is given below. According to [22], it is generated with a correlation coefficient for each pairs of clocks fixed at $\rho_{ij} = 0.10$:

$$\boldsymbol{R} = \begin{pmatrix} r_{11} & r_{12} & r_{13} & r_{14} \\ r_{12} & r_{22} & r_{23} & r_{24} \\ r_{13} & r_{23} & r_{33} & r_{34} \\ r_{14} & r_{24} & r_{34} & r_{44} \end{pmatrix} = \begin{pmatrix} 2.085 & 0.153 & 2.237 & 0.297 \\ 0.153 & 1.143 & 1.744 & 0.234 \\ 2.237 & 1.744 & 239.62 & 3.524 \\ 0.297 & 0.234 & 3.524 & 4.064 \end{pmatrix}$$

The computed correlation coefficients associated with $\boldsymbol{R}$ are close to 0.10:

$$\boldsymbol{\rho} = \begin{pmatrix} \rho_{11} & \rho_{12} & \rho_{13} & \rho_{14} \\ \rho_{12} & \rho_{22} & \rho_{23} & \rho_{24} \\ \rho_{13} & \rho_{23} & \rho_{33} & \rho_{34} \\ \rho_{14} & \rho_{24} & \rho_{34} & \rho_{44} \end{pmatrix} = \begin{pmatrix} 1.000 & 0.099 & 0.100 & 0.102 \\ 0.099 & 1.000 & 0.105 & 0.109 \\ 0.100 & 0.105 & 1.000 & 0.113 \\ 0.102 & 0.109 & 0.113 & 1.000 \end{pmatrix}$$

The covariance matrix $\boldsymbol{S}$ corresponding to $\boldsymbol{R}$ can be computed using the relationship between $\boldsymbol{R}$ and $\boldsymbol{S}$:

$$\boldsymbol{S} = \boldsymbol{H}^T \cdot \boldsymbol{R} \cdot \boldsymbol{H} = \begin{pmatrix} s_{11} & s_{12} & s_{13} \\ s_{12} & s_{22} & s_{23} \\ s_{13} & s_{23} & s_{33} \end{pmatrix} = \begin{pmatrix} 5.555 & 3.686 & 2.480 \\ 3.686 & 4.739 & 2.050 \\ 2.480 & 2.050 & 236.636 \end{pmatrix},$$

where

$$\boldsymbol{H} = \begin{pmatrix} +1 & 0 & 0 \\ 0 & +1 & 0 \\ 0 & 0 & +1 \\ -1 & -1 & -1 \end{pmatrix}.$$

Now, using the 5 different methods, the results for $\boldsymbol{R}$ and $\boldsymbol{\rho}$ are summarized in Tables 9 and 10 below:

Method	$\hat{\boldsymbol{R}}$	$\hat{\boldsymbol{\rho}}$
True Value $\boldsymbol{R}$, $\boldsymbol{\rho}$	$\begin{pmatrix} 2.085 & 0.153 & 2.237 & 0.297 \\ 0.153 & 1.143 & 1.744 & 0.234 \\ 2.237 & 1.744 & 239.62 & 3.524 \\ 0.297 & 0.234 & 3.524 & 4.064 \end{pmatrix}$	$\begin{pmatrix} 1.000 & 0.099 & 0.100 & 0.102 \\ 0.099 & 1.000 & 0.105 & 0.109 \\ 0.100 & 0.105 & 1.000 & 0.113 \\ 0.102 & 0.109 & 0.113 & 1.000 \end{pmatrix}$
Method 1 Three Cornered Hat	$\begin{pmatrix} 2.817 & 0.000 & 0.000 & 0.000 \\ 0.000 & 2.000 & 0.000 & 0.000 \\ 0.000 & 0.000 & 233.90 & 0.000 \\ 0.000 & 0.000 & 0.000 & 2.739 \end{pmatrix}$	$\begin{pmatrix} 1.000 & 0.000 & 0.000 & 0.000 \\ 0.000 & 1.000 & 0.000 & 0.000 \\ 0.000 & 0.000 & 1.000 & 0.000 \\ 0.000 & 0.000 & 0.000 & 1.000 \end{pmatrix}$
Method 2 (Tavella)	$\begin{pmatrix} 2.265 & 0.625 & -0.134 & -0.205 \\ 0.625 & 1.907 & -0.334 & 0.024 \\ -0.134 & -0.334 & 234.70 & 0.471 \\ -0.205 & 0.024 & 0.471 & 2.880 \end{pmatrix}$	$\begin{pmatrix} 1.000 & 0.301 & 0.006 & 0.080 \\ 0.301 & 1.000 & 0.016 & 0.010 \\ 0.006 & 0.016 & 1.000 & 0.018 \\ 0.080 & 0.010 & 0.018 & 1.000 \end{pmatrix}$
Method 3 (Torcasso)	$\begin{pmatrix} 2.435 & 0.805 & -0.135 & -0.035 \\ 0.805 & 2.098 & -0.326 & 0.205 \\ -0.135 & -0.326 & 234.53 & 0.470 \\ -0.035 & 0.205 & 0.470 & 3.051 \end{pmatrix}$	$\begin{pmatrix} 1.000 & 0.356 & -0.006 & -0.013 \\ 0.356 & 1.000 & -0.015 & 0.081 \\ -0.006 & -0.015 & 1.000 & 0.018 \\ -0.013 & 0.081 & 0.018 & 1.000 \end{pmatrix}$
Method 4 (Galindo)	$\begin{pmatrix} 1.859 & 0.003 & 0.035 & -0.011 \\ 0.003 & 1.069 & -0.382 & 0.003 \\ 0.035 & -0.382 & 235.44 & 1.241 \\ -0.011 & 0.003 & 1.241 & 3.675 \end{pmatrix}$	$\begin{pmatrix} 1.000 & 0.002 & 0.002 & -0.004 \\ 0.002 & 1.000 & -0.024 & 0.001 \\ 0.002 & -0.024 & 1.000 & 0.042 \\ -0.004 & 0.001 & 0.042 & 1.000 \end{pmatrix}$
Method 5 (Ruiz)	$\begin{pmatrix} 1.867 & 0.003 & 0.425 & 0.000 \\ 0.003 & 1.062 & 0.000 & 0.006 \\ 0.425 & 0.000 & 236.21 & 1.633 \\ 0.000 & 0.006 & 1.633 & 3.688 \end{pmatrix}$	$\begin{pmatrix} 1.000 & 0.002 & 0.020 & 0.000 \\ 0.002 & 1.000 & 0.000 & 0.003 \\ 0.020 & 0.000 & 1.000 & 0.055 \\ 0.000 & 0.003 & 0.055 & 1.000 \end{pmatrix}$

Table 9. Comparison of the covariance and correlation matrices for the five approaches

Just by looking at the table, is difficult to say which approach provides results closer to the true values of $\boldsymbol{R}$ and $\boldsymbol{\rho}$. In order to compare them, the proposed *MOP*'s are presented in Table 10:

	MOP_1	MOP_2	MOP_3
Method 1	56.4062	0.0659	35.7756
Method 2	46.0122	0.1185	26.2352
Method 3	47.7893	0.1148	28.0140
Method 4	32.4091	0.0636	17.6589
Method 5	21.8667	0.0518	11.8007

Table 10. Comparison of the *MOP*'s obtained by each method

For all *MOP´*s, a smaller value indicates a better result. The fifth method (the new one) seems to provide better results for all *MOP´*s, i.e., it dominates regardless of *MOP*.

C. TEST N°2, RANDOM COVARIANCE MATRIX SIMULATION

In order to check if the results in the previous section are just a lucky outcome coming from a particular favorable set of data, a simulation of similar problems is made in this section.

In order to reduce the variance of the results, common random numbers are used among the 5 different methods. The simulation is performed for an ensemble of 4 correlated clocks presenting similar characteristics. It consists of the following phases:

- Generation of the absolute covariance matrices $\boldsymbol{R}_{4\times4}$.
- Computation of the relative covariance matrices $\boldsymbol{S}_{3\times3}$.
- Estimation of the absolute covariance matrices $\hat{\boldsymbol{R}}_1$, $\hat{\boldsymbol{R}}_2$, $\hat{\boldsymbol{R}}_3$, $\hat{\boldsymbol{R}}_4$ and $\hat{\boldsymbol{R}}_5$ from $\boldsymbol{S}$ using the 5 different approaches.
- Computation of the measures of performance MOP_1, MOP_2, and MOP_3
- Analyze and present the results.

The random parameters used in the simulation correspond to the ones expected in an ensemble of atomic clocks, but with special attention to the correlation among them since this is one of the objectives of the present work. The absolute covariance matrix $\boldsymbol{R}$ is obtained by generating the variance terms (main diagonal) and desired correlation coefficients between each pair of clocks. A total of 40000 runs of simulations are performed with the following distribution for the random parameters:

- r_{11}, r_{22}, r_{33} and r_{44} uniformly distributed between 1 and 20 in arbitrary units.
- ρ_{12}, ρ_{13}, ρ_{14}, ρ_{23}, ρ_{24} and ρ_{34} uniformly distributed between 0 and 0.1

The results for the 3 *MOP*'s are shown in Figures 4, 5 and 6. They represent the histograms corresponding to the distribution of each *MOP* for the different approaches tested.

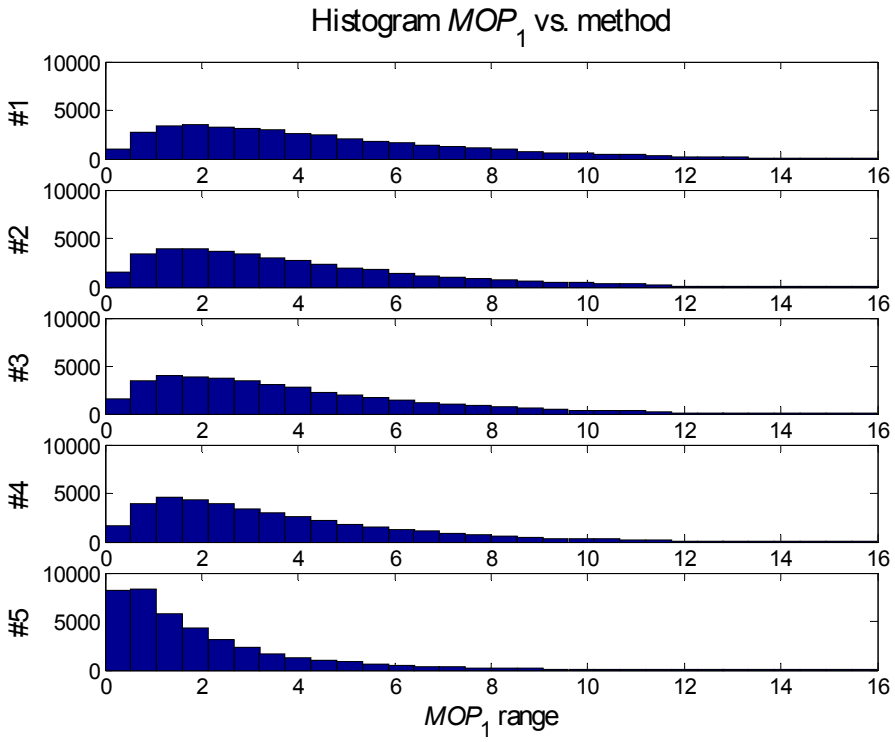

Figure 4. Comparison of 1st *MOP*

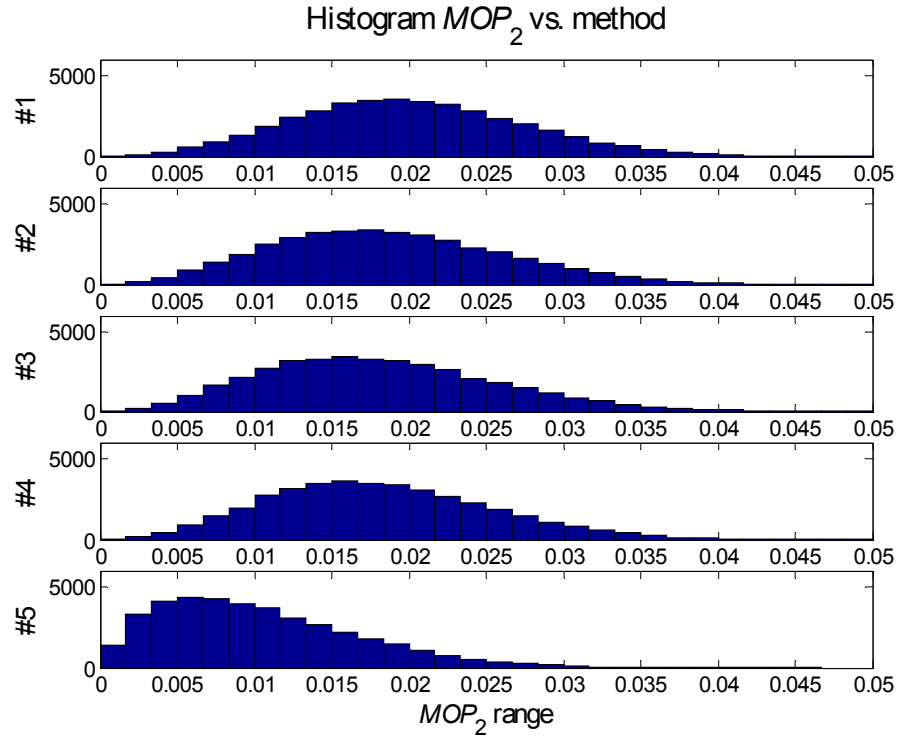

Figure 5. Comparison of 2nd *MOP*

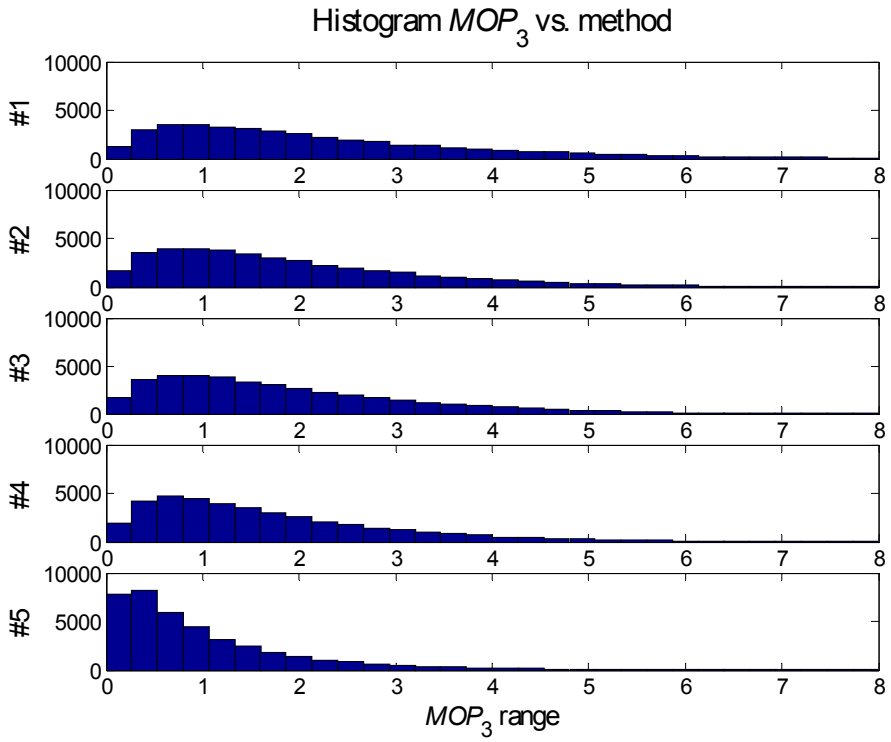

Figure 6. Comparison of 3rd *MOP*

The mean and standard deviation obtained for the tree *MOP*'s is shown in Tables 11, 12 and 13:

	MOP 1				
Method	#1	#2	#3	#4	#5
Mean, $\bar{X}$	4.4080	3.8508	3.8239	3.5891	2.0172
Std. Dev, $\hat{s}$	3.0496	2.7553	2.7427	2.6750	1.9999

Table 11. Summary table for *MOP* 1

	MOP's 2				
Method	#1	#2	#3	#4	#5
Mean, $\overline{X}$	0.0200	0.0199	0.0182	0.0181	0.0104
Std. Dev, $\hat{s}$	0.0073	0.0323	0.0080	0.0072	0.0065

Table 12. Summary table for *MOP* 2

	MOP 3				
Method	#1	#2	#3	#4	#5
Mean, $\overline{X}$	2.2315	1.8788	1.8819	1.7011	1.0165
Std. Dev, $\hat{s}$	1.6399	1.3465	1.3520	1.2708	0.9856

Table 13. Summary table for *MOP* 3

The three tables show that the proposed approach not only provides smaller expected values for all *MOP*'s, which means that the results are more accurate, but also provides smaller standard deviations, so the results are more consistent as well.

D. TEST N°3, TEST OF SENSITIVITY OF THE NEW PROPOSAL

This test tries to study the dynamical behavior of the proposed method. In this case, five clocks are simulated. For each run, an absolute covariance matrix $\boldsymbol{R}$ is first generated. Then, the relative covariance matrix $\boldsymbol{S}$ is computed and finally $\boldsymbol{R}$ is estimated by solving the minimization problem given in (2.43). The variance terms corresponding to the elements of the main diagonal of $\boldsymbol{R}$ are simulated according the following predefined pattern:

$$
\begin{aligned}
r_{11} &= 15 + 10 \cdot \cos(\frac{2 \cdot \pi \cdot t}{1024}); \\
r_{22} &= 20 - 8 \cdot \cos(\frac{2 \cdot \pi \cdot t}{1024} + \frac{\pi}{2}) \\
r_{33} &= 30 - \frac{20 \cdot t}{1024} \\
r_{44} &= 5 + 25 \cdot \left(\frac{t}{1024} \right)^2 \\
r_{55} &= 15 + 10 \cdot \cos(\frac{2 \cdot \pi \cdot t}{1024} - \frac{3 \cdot \pi}{2}); \\
t &= \{0, 1, 2, ..., 1024\}
\end{aligned}
\tag{3.4}
$$

Then, for $i \neq j$, the rest of the elements of $\boldsymbol{R}$ are computed using:

$$
r_{ij} = \rho_{ij} \cdot \sqrt{r_{ii} \cdot r_{jj}} \tag{3.5}
$$

Where the correlation coefficients ρ_{ij} are fixed at 0.1.

The output of the algorithm is the estimation of the absolute covariance matrix $\hat{\boldsymbol{R}}$. The idea behind the simulation is to test the sensitivity of the algorithm in order to check if small changes in the input parameters might produce big changes in the output. The total number of runs in this simulation is fixed to 2^{10}

The usual approach to select the weight for each clock is to make the weights inversely proportional to the computed variance of each clock, as shown in section II B. In Figures 7 and 8, the simulated and computed variance terms (diagonal elements of the covariance matrix) and the corresponding weights are shown. The true value used in the simulation has also been drawn in a solid line.

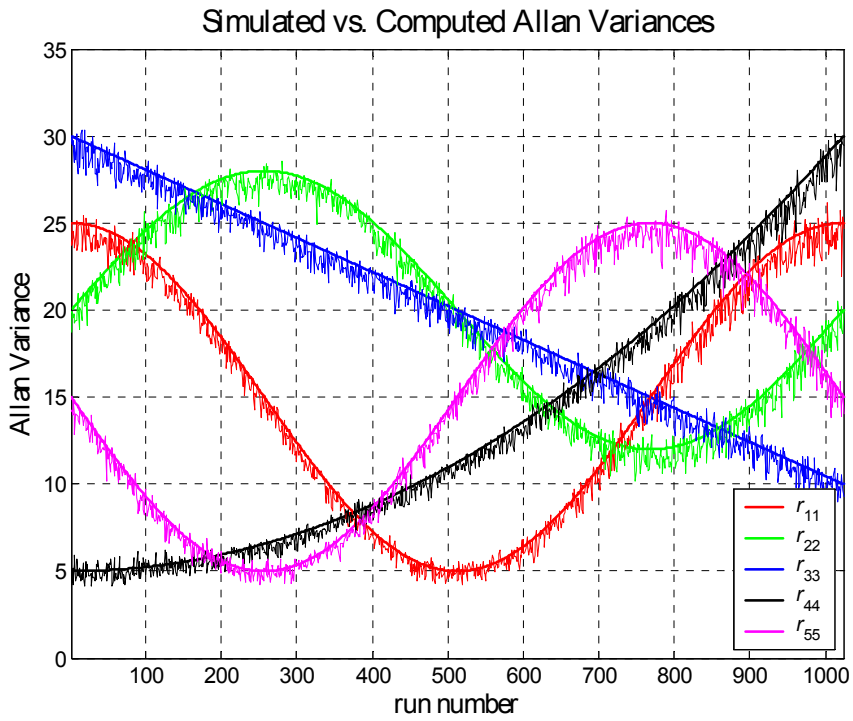

Figure 7. Simulated vs. Computed Allan variances

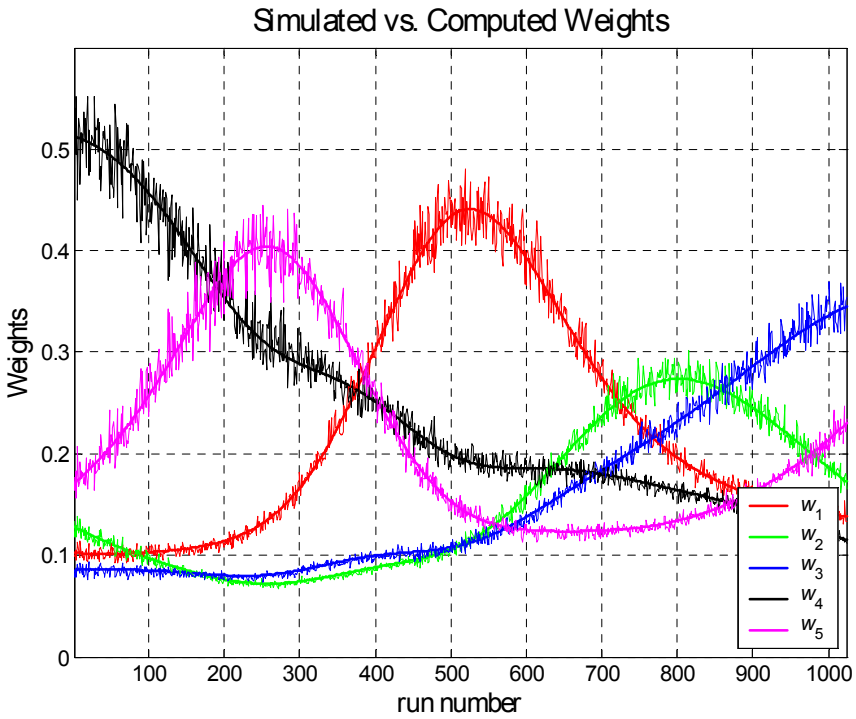

Figure 8. Simulated vs. Computed Optimal Weights

In all cases, the algorithm converged to a solution close to the true value and no extra runs with different initial conditions are needed. The mean value and its standard deviation for the relative error of both Allan variances and weights are presented in Tables 14 and 15

Allan Var	Clock #1	Clock #2	Clock #3	Clock #4	Clock #5
Mean rel. err.	+0.0287	+0.0255	+0.0256	+0.0310	+0.0304
Std rel. err.	+0.0434	+0.0318	+0.0327	+0.0478	+0.0424

Table 14. Summary of relative errors in Allan variance

Weights	Clock #1	Clock #2	Clock #3	Clock #4	Clock #5
Mean rel. err.	+0.0022	+0.0060	+0.0059	-0.0005	+0.0003
Std rel. err.	+0.0419	+0.0390	+0.0386	+0.0453	+0.0461

Table 15. Summary of relative errors in Weights

The histograms showing the distribution of relative errors, grouped by clock, have been included in Figure 9.

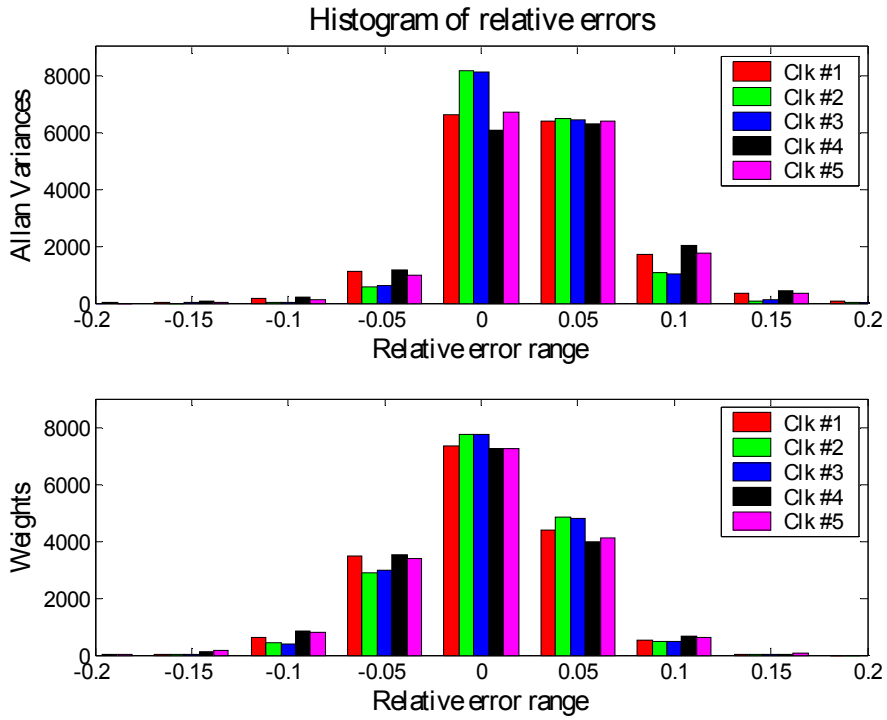

Figure 9. Relative errors in Allan variances and Weights

The results are clearly acceptable. In 77% of the runs the errors are smaller than 0.05%, and in 98% of the runs the errors are smaller than 0.10%

One final note about the algorithm is that, in general, it seems to underdetermine the Allan variances associated with each clock. However, since this effect happens with all of the clocks, the final result is that for the calculations of the weights the effect is compensated. It can be seen that in Figure 7, the computed variances are below the true values identified by the solid line. However, in Figure 8 the computed weights are more centered near the true values, which is beneficial since they are the values needed to characterize each clock.

E. TEST N°4, PHASE SIMULATION

In this case, a complete simulation is carried out to analyze the whole process. The differences in time among the different pairs of clocks are generated in advance in order to be later used as the input data for the program. The process of generating the simulated data involves some decisions about the kind of noise that is going to be introduced in the system and which requires a close study. Since this simulation involves several stages, all of them need to be checked. In particular, whenever intermediate results are obtained, they are compared to the true values of the same parameters. The steps that will be analyzed and checked in detail are:

- Generation of the appropriate type of noise process.
- Generation of the fractional frequency deviations and time differences between pairs of clocks.
- Estimation of the relative covariance matrix ***S*** associated with the ensemble.
- Estimation of the absolute covariance matrix ***R*** associated with the ensemble.
- Estimation of the weight associated with each clock.

1. Generation of the Appropriate Type of Noise Process.

Atomic clocks may show, in general, the five different types of noise presented in chapter I. They are characterized by the spectral components present, that is by the Power Spectral Density (PSD). The different types are easily identified in the frequency domain by the slope of the PSD of the fractional frequency deviation $S_y(f)$ in a logarithmic plot. Fortunately, there is also a correspondence between the frequency domain and the time domain. This correspondence implies that the type of noise can also

be identified in the time domain by plotting the Allan variance $\sigma_y^2(\tau)$ (or Allan deviation, $\sigma_y(\tau)$) or Modified Allan variance $Mod\ \sigma_y^2(\tau)$) as a function of the averaging time τ.

The first step in this simulation is related to the generation of time data corrupted with additive noise of specific spectral characteristics. Table 16 summarizes the 5 types of noise and its characterization in both domains, time and frequency, and includes the results shown in Tables 1 and 8.

Noise Process	Slope Characteristics in Log-Log Plot				
	Frequency Domain		Time Domain		
	$S_y(f)$	$S_x(f)$	σ_y^2	σ_y	M σ_y
Slope	α	β	μ	$\mu/2$	μ'
Random Walk Frequency Modulation	-2	-4	1	½	1/2
Flicker Frequency Modulation	-1	-3	0	0	0
White Frequency Modulation	0	-2	-1	-1/2	-1/2
Flicker Phase Modulation	1	-1	-2	-1	-1
White Phase Modulation	2	0	-2	-1	-1/2

Table 16. Noise processes used in modeling frequency instability

The five types of noise processes are first generated using the algorithm suggested in [29]. The noise is normalized so that in all cases the Allan variance corresponding to an averaging time of $\tau = 1$ is equal to 1.

In order to test if the generated noise agrees with the desired characteristics, a straight line is fitted to the log-log plot of both the power spectral density of the fractional

frequency deviations $S_y(f)$ and to the Allan deviation $\sigma_y(\tau)$ as a function of the averaging factor. The results for the theoretical and computed slopes and the corresponding Figures 11 and 12 are also shown below.

Noise Type	Freq. Domain		Time Domain	
	Theoretical	Computed	Theoretical	Computed
RWFM	-2	-1.80	1/2	0.48
FFM	-1	-1.01	0	-0.01
WFM	0	-0.00	-1/2	-0.51
FPM	+1	0.78	-1	-0.88
WPM	+2	1.79	-1	-1.00

Table 17. Theoretical and computed slopes for the different noise processes

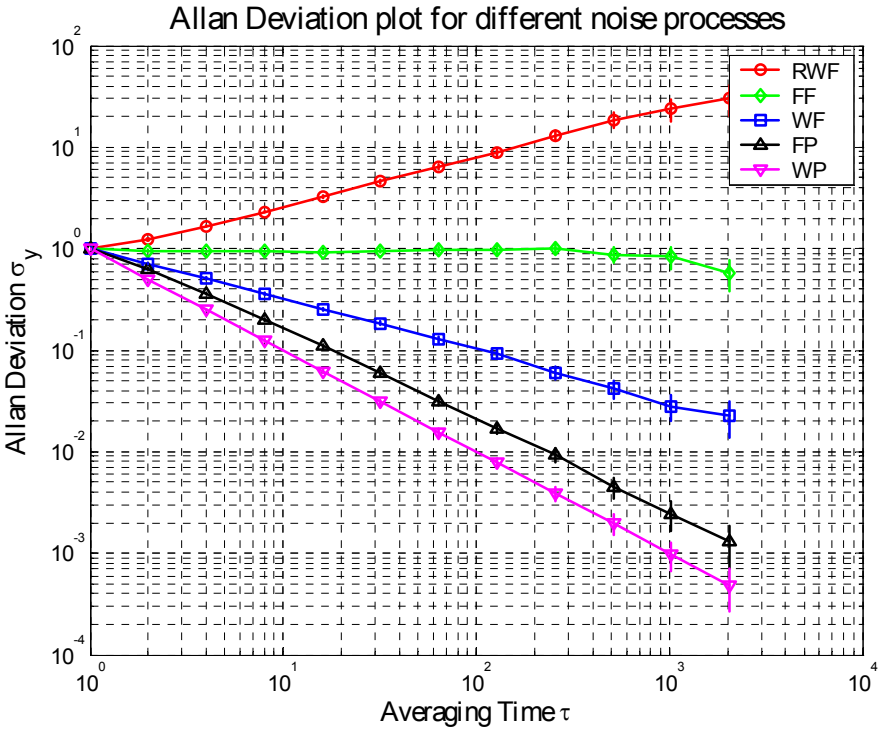

Figure 10. Simulated noise processes and corresponding Allan deviation plot

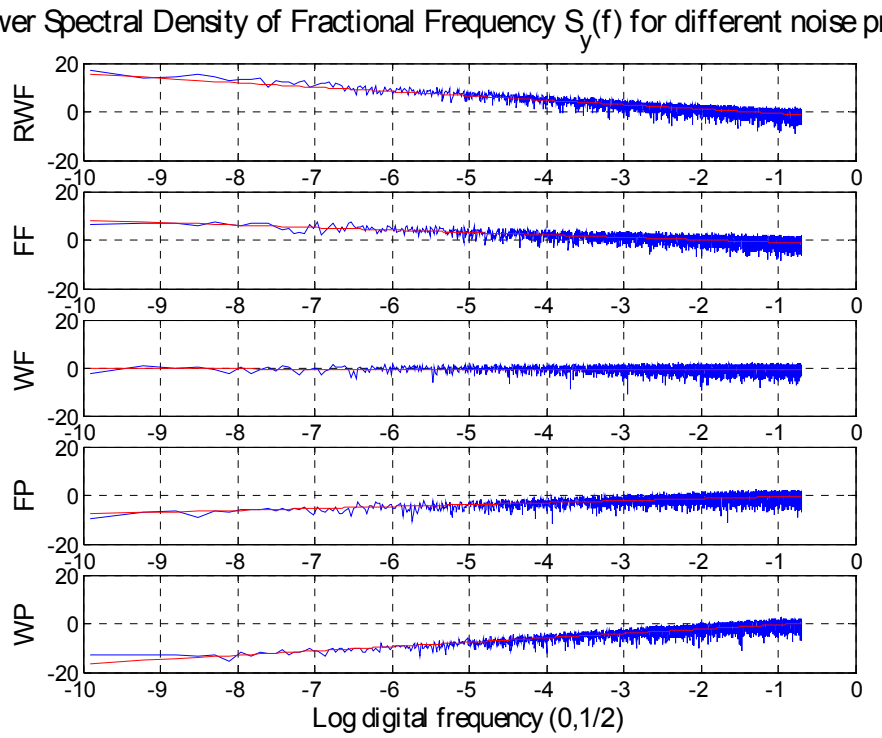

Figure 11. Simulated noise processes and corresponding Power Spectral Density plot

For Cesium Time Standards located in The Royal Observatory of the Spanish Navy, the expected type of noise for averaging time in the order of weeks or greater is Random Walk Frequency Modulation[6]. Consequently, this is the type of noise that is used in the simulation for all clocks.

2. Generation of the Fractional Frequency Deviations and Time Differences Between Pairs of Clocks

Once the proper type of noise has been generated for each clock, the next step consists of the generation of the absolute fractional frequencies and time differences between each single time standard and an ideal clock. Once these fractional frequencies are known, the absolute time differences between each clock and an ideal clock can be computed by numerical integration of the fractional frequencies. The last step to finally compute the relative time differences between each pair of real clocks is done by pairwise

subtraction of the absolute time differences previously obtained. These relative time differences among the real clocks will be the required input to the program.

The absolute and relative fractional frequency fluctuations and time differences associated with the ensemble are shown in Figures 12 to 15. Since the time origin does not affect stability, all of the clocks are initially supposed to be perfectly synchronized.

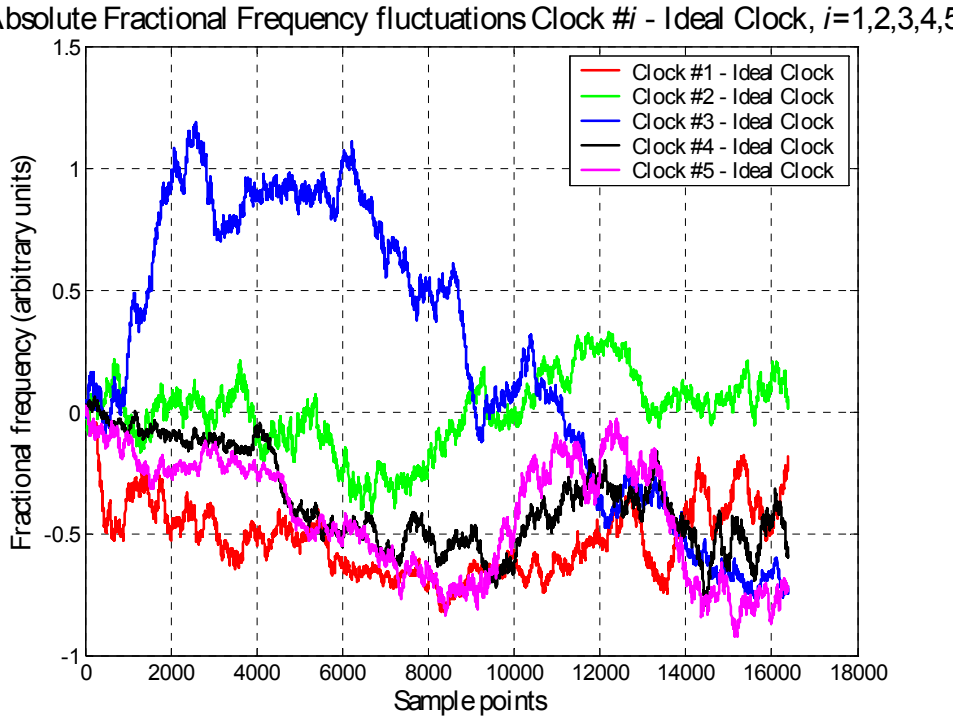

Figure 12. Absolute Fractional Frequency fluctuations

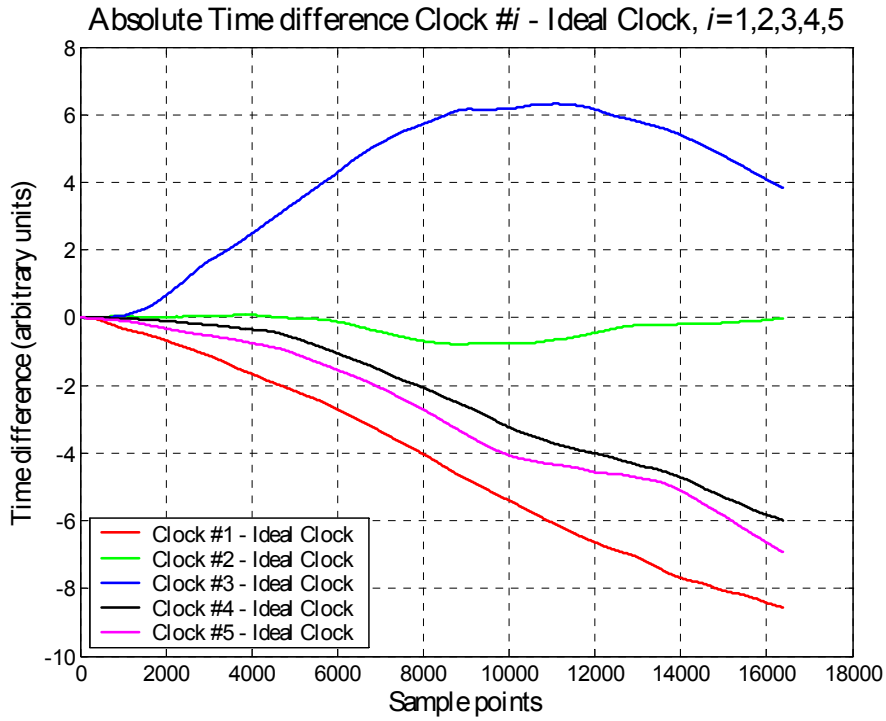
Absolute Time difference Clock #i - Ideal Clock, i=1,2,3,4,5
Time difference (arbitrary units)
Sample points
Clock #1 - Ideal Clock
Clock #2 - Ideal Clock
Clock #3 - Ideal Clock
Clock #4 - Ideal Clock
Clock #5 - Ideal Clock

Figure 13. Absolute Time differences

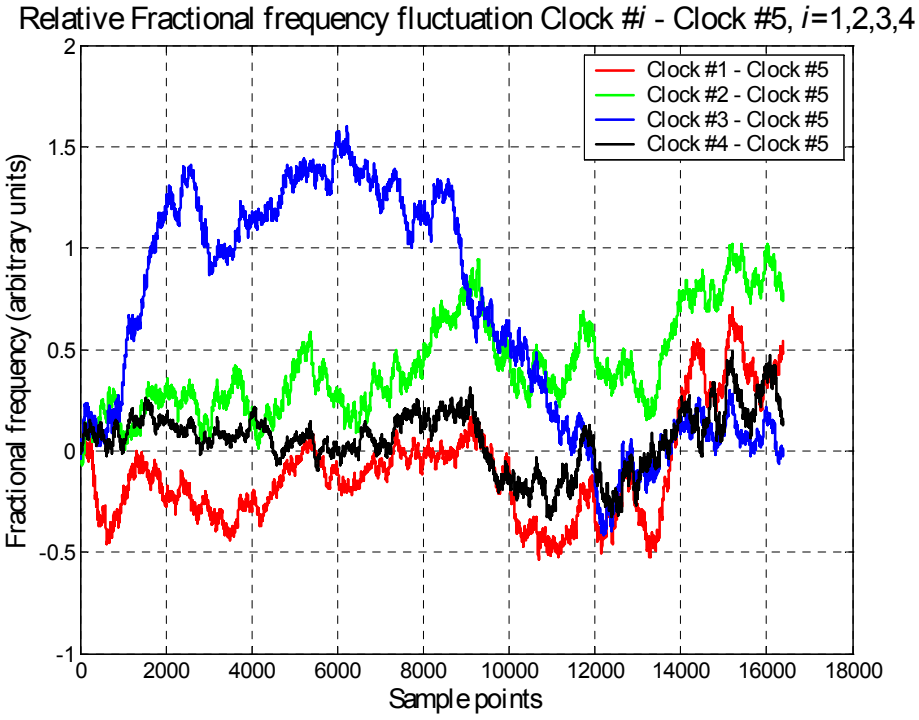
Relative Fractional frequency fluctuation Clock #i - Clock #5, i=1,2,3,4
Fractional frequency (arbitrary units)
Sample points
Clock #1 - Clock #5
Clock #2 - Clock #5
Clock #3 - Clock #5
Clock #4 - Clock #5

Figure 14. Relative Fractional Frequency fluctuations

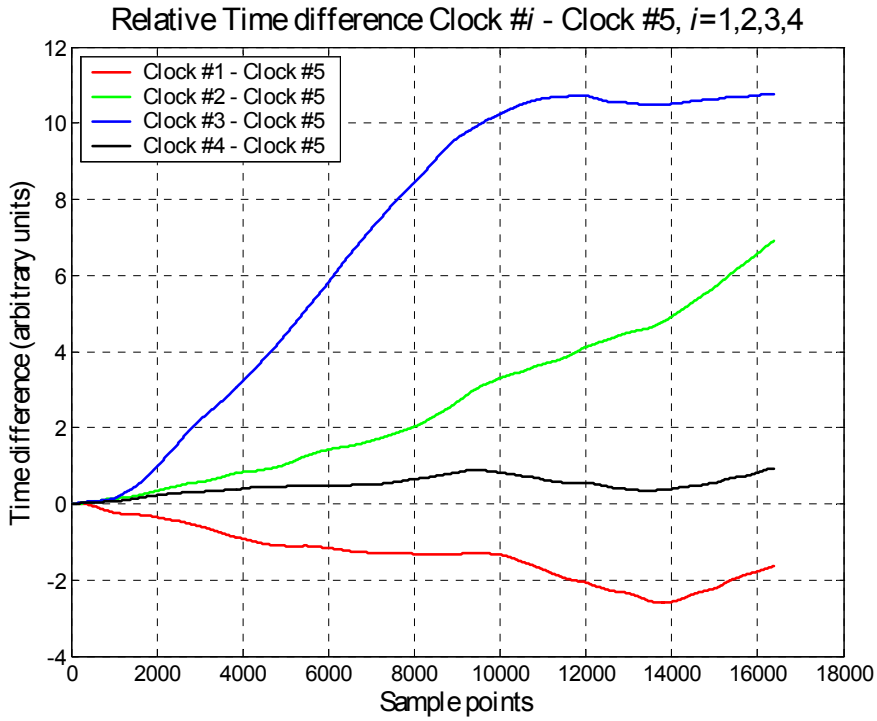

Figure 15. Relative Time differences

The data shown in Figure 12 is the input data required to characterize each clock; it represents how the time scales provided by each clock diverge with time. The laboratory data available for this study is similar to the data shown, but coming from real atomic clocks instead of simulated.

3. Estimation of the Relative Covariance Matrix *S* Associated with the Ensemble

Once the time series containing the time differences between each of the clocks and the reference is known, the relative Allan (co)variance matrix ***S*** needs to be computed. In order to do so, some decisions need to be made in advance because there is a trade off between the number of sample points to use in each computation of the matrix ***S*** and the desired accuracy in the time location of the changes in stability associated with each clock. If the number of sample points used in the computation of ***S*** is too big, then the matrix ***S*** will present a smooth variation with time and changes in the stability of a

particular clock may be either filtered out or may not be detected. On the other hand, if the number of sample points used in the computation of $\boldsymbol{S}$ is too small, the matrix $\boldsymbol{S}$ will be very noisy, and consequently the later computation of the absolute covariance matrix $\boldsymbol{R}$ will be affected.

In this simulation, several choices in the sample size are used to test this effect, in particular, sample sizes of 100, 200 and 500 data points are used to compute $\boldsymbol{S}$. The effect on sample size is shown in Figure 16, along with the theoretical or true value for the diagonal and off-diagonal terms of the matrix $\boldsymbol{S}$. As expected, the oscillations of the computed value around the true one decrease in amplitude with the number of data points used in the computation.

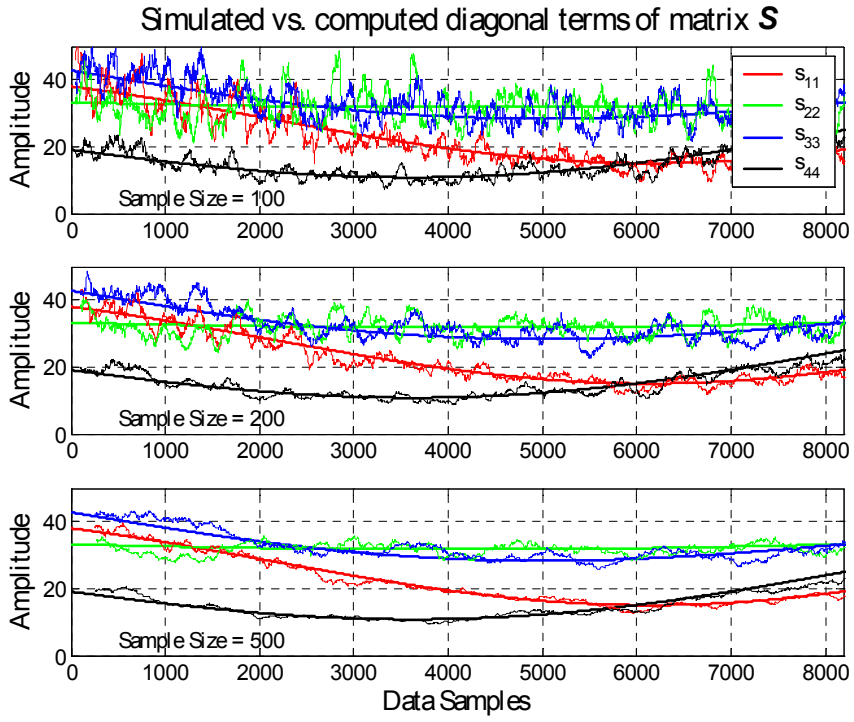

Figure 16. Diagonal terms of matrix $\boldsymbol{S}$

In order to solve the minimization problem to find the diagonal terms of the matrix $\boldsymbol{R}$, the complete $\boldsymbol{S}$ matrix must be first computed. The off-diagonal terms of $\boldsymbol{S}$ are plotted in Figure 17.

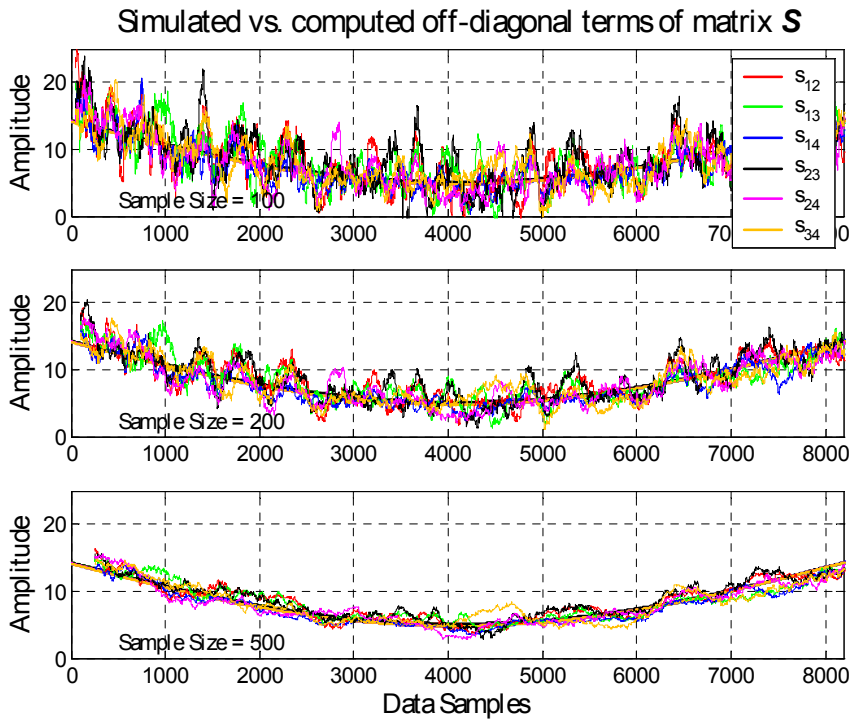

Figure 17. Off-diagonal terms of matrix ***S***

It is no surprise that all of the off-diagonal terms of the matrix ***S*** are very similar. The reason is that, for the case of five clocks, all of them are formed as a linear combination of off-diagonal terms of the matrix ***R*** (which are small) plus the variance term corresponding to the clock that is chosen as reference (r_{55}), which can be several orders of magnitude greater than the off-diagonal terms of ***R***.

The results for the matrix ***S*** shown in Figures 13 and 14 are the input values for the algorithm that obtains the diagonal terms of ***R***. Noise enters into the estimation process of ***S,*** and is consequently carried to the end of the process. This is the reason why accurate values for ***R*** are difficult to achieve in practice.

4. Estimation of the Absolute Covariance matrix *R* Associated with the Ensemble

The last step in the simulation corresponds to the minimization problem that allows the computation of the variance terms associated with each clock. This process is carried out in two steps to help the convergence of the method. In the first step the three cornered-hat method is used to find an approximate solution. This solution is passed to the method to be used as an initial solution in the algorithm described in chapter II.

The final results, again, depend on the sample size used. In general, there is a good agreement between the simulated values for the variance terms and the computed values as is shown in Figure 18.

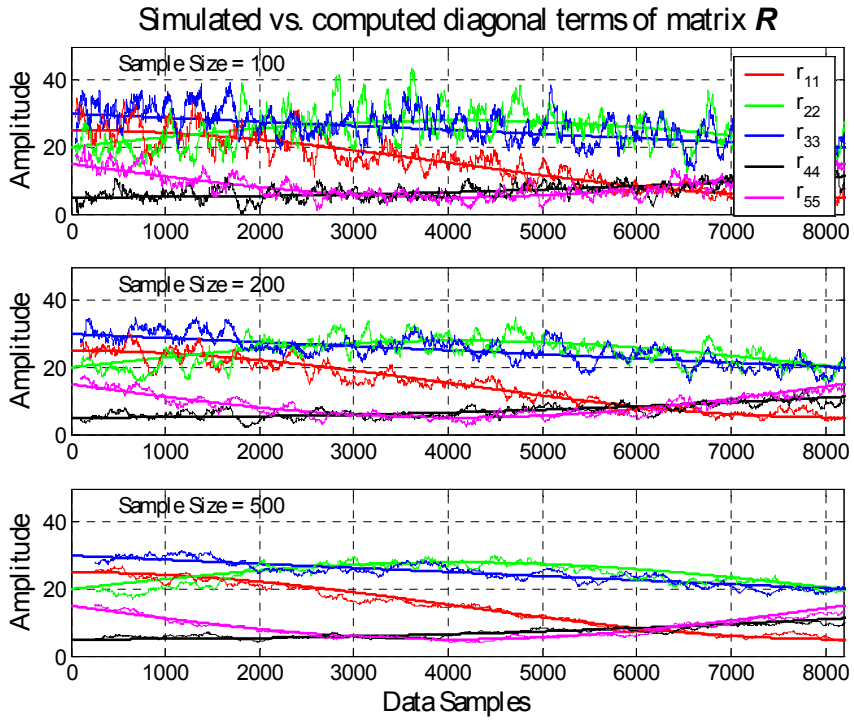

Figure 18. Diagonal terms of matrix ***R***

5. Estimation of the Weights Associated with Each Clock.

This is a straightforward step, since the optimal value for the weights associated with each clock is proportional to the inverse of its variance., After some manipulation of the data plotted in Figure 15, the weights are computed and plotted in Figure 16.

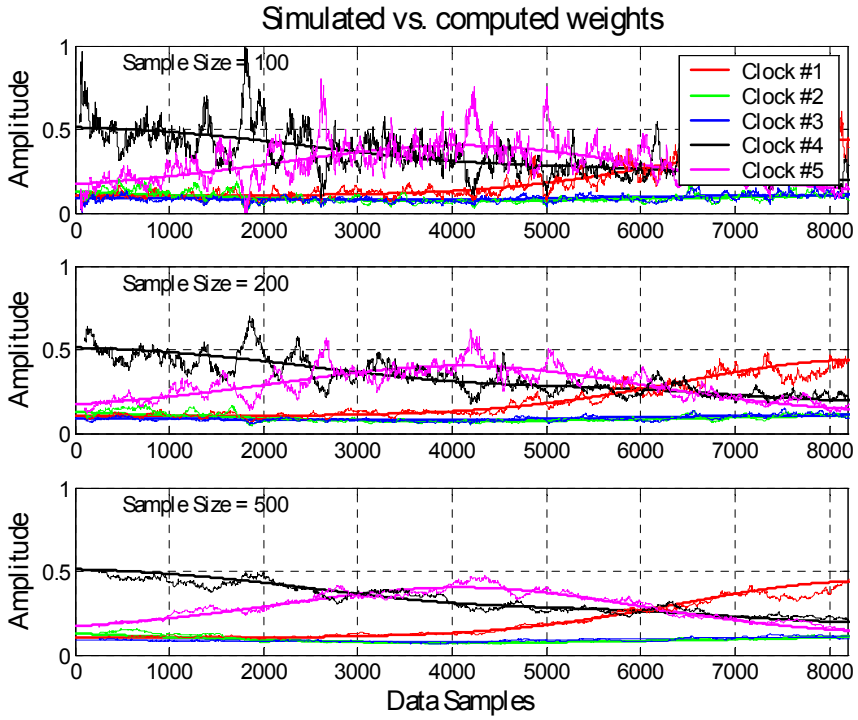

Figure 19. Simulated vs. computed weights

Figure 19 shows that there is a trade off between the number of samples used in the computation and the time resolution obtained. If the number of samples is too small, then the result is noisy. On the other hand, if the number of samples is too big, time changes in the behavior of the clocks are not immediately detected.

THIS PAGE INTENTIONALLY LEFT BLANK

IV. APPLICATION OF THE METHOD TO REAL DATA

A. OVERVIEW

In this chapter, a data file obtained from the Royal Observatory of the Spanish Navy is analyzed. The file consists of differences in time between 4 atomic clocks and another atomic clock of the same characteristics chosen as a reference. The measurement noise is negligible compared to the noise introduced by the atomic clocks, so only 4 columns of data are required to perform the study. For the rest of the chapter, the clocks will be referred to as Clock #1, Clock #2, … and Clock #5. The data file has the following structure, where the differences in time are expressed in nanoseconds:

Day	Clock #1- Clock #5	Clock #2- Clock #5	Clock #3- Clock #5	Clock #4- Clock #5
0	…….	…….	…….	…….
5	…….	…….	…….	…….
…	…….	…….	…….	…….
1245	…….	…….	…….	…….

Table 18. Structure of the data file

B. INITIAL EXPLORATION OF THE DATA

The raw data contained in the file is shown in Figure 20. The parabolic shape of the data show the typical effect present in Cesium Standards of a constant linear drift in frequency, which is equivalent to a parabolic drift in time. These are systematic effects that must be estimated and subtracted from the data.

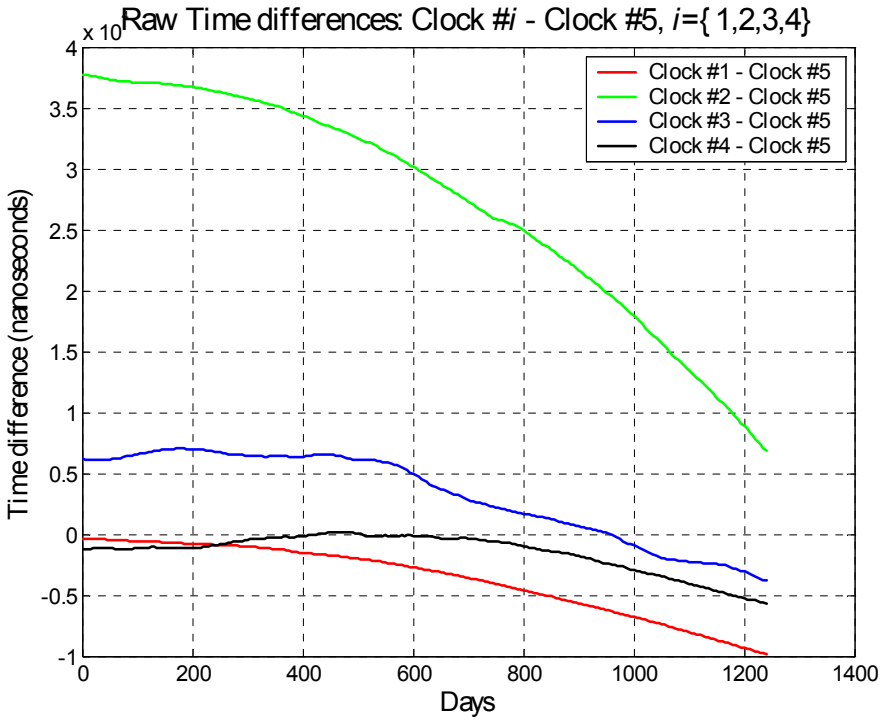

Figure 20. Raw Time differences between clocks

C. INITIAL FILTERING

Before using the data, it is necessary to preprocess it in two ways. First, the initial time difference between clocks is just a constant term that plays no role in the stability characteristics of each clock, so it is subtracted so that all of the clocks can be considered to be perfectly synchronized in time at the beginning of the analysis. Second, the deterministic effects associated with a constant drift in frequency can also be filtered by fitting a second order polynomial to the data and subtracting it from the raw data. When both processes are performed, the noise processes appear evident. The time residuals and associated fractional frequency deviations are shown in Figures 21 and 22; they are the data necessary to carry out the subsequent analysis.

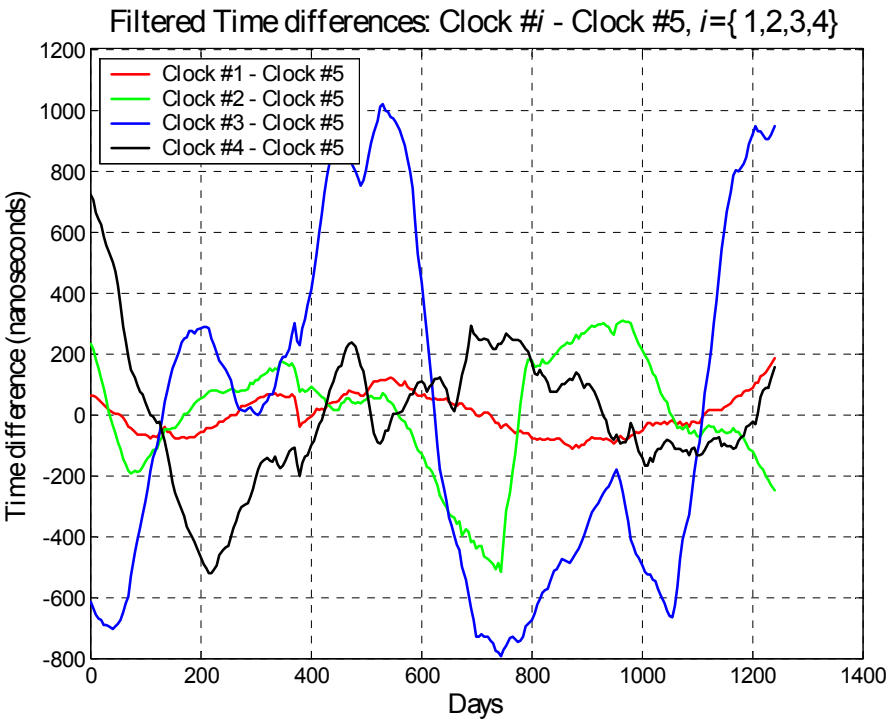

Figure 21. Filtered Time differences between clocks

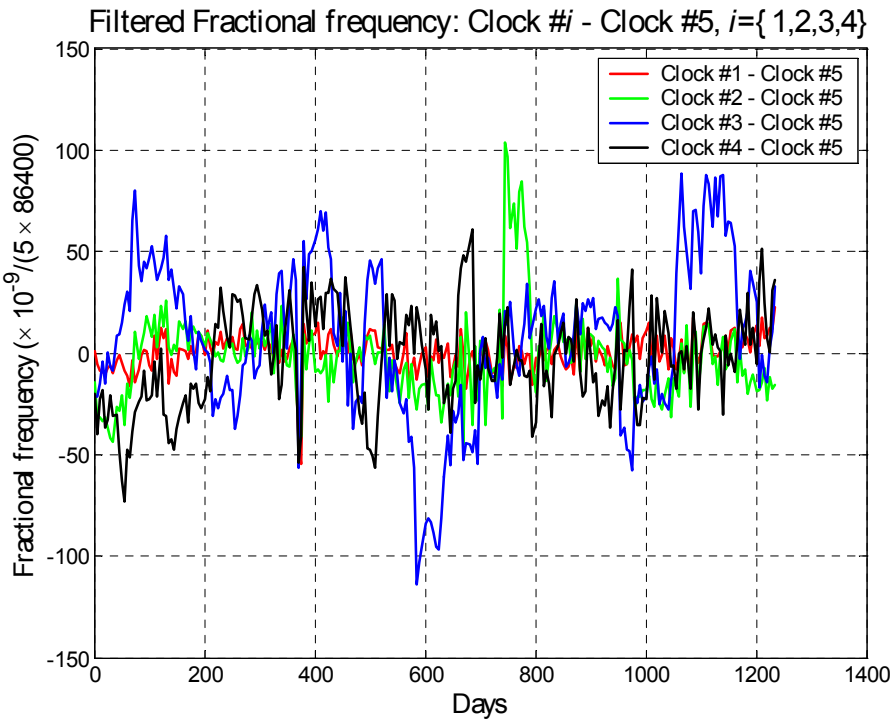

Figure 22. Filtered Fractional frequency between clocks

D. CHARACTERIZATION OF THE ENSEMBLE

The final step consists of the application of the new method that has been developed in this thesis. The input data are the data shown in Figure 19. In order to capture non stationary changes in the stability characteristics of the clocks, a window length must be chosen to compute the Allan variances of each clock for the period of time corresponding to the window. For the data provided, a window length of 128 samples is a good trade off between time accuracy and convergence of the method.

Figure 23 provides the computed Allan deviation for the data file provided for this work for an averaging time of $\tau = 5$ days.

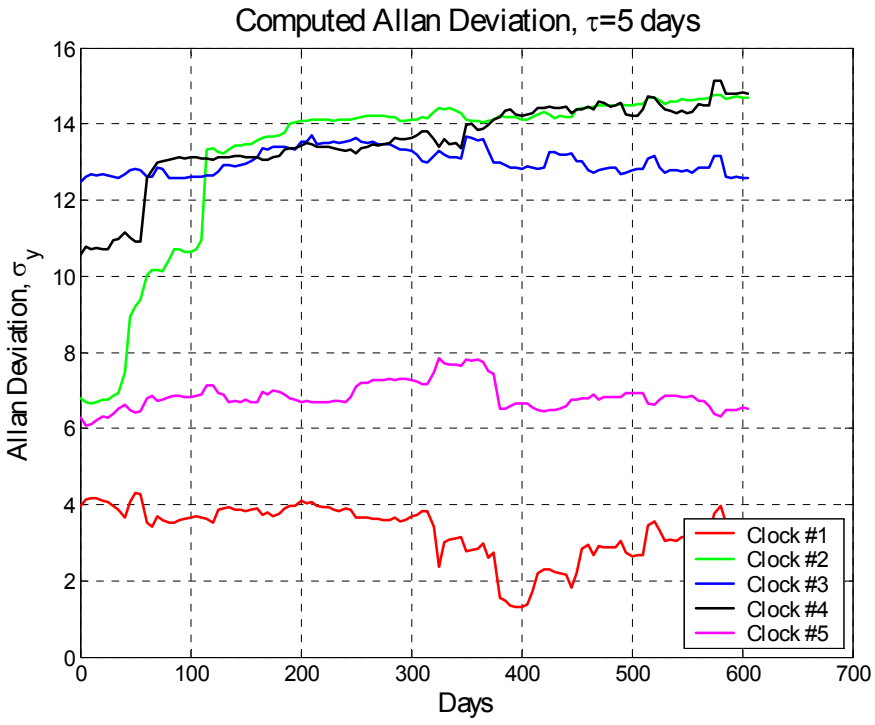

Figure 23. Computed Allan deviation for the ensemble

For comparison purposes, the same available data file of time differences among the clocks of the ensemble is also analyzed using a method based on the classical Three-Cornered Hat approach. For this particular case, no negative variances are found and consequently, the results are close to the ones obtained with the approach presented in this thesis However, when the window width is changed to 64 samples instead of 128, the Three-Cornered Hat approach provides no results whatsoever since some of the computed variances are negative. The results are shown in Figure 24.

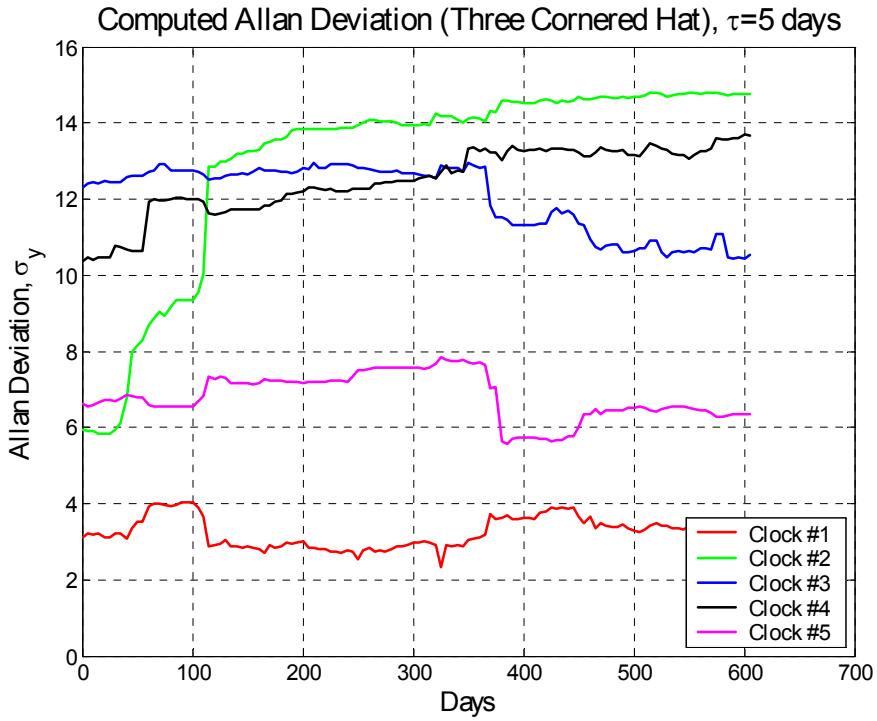

Figure 24. Computed Allan deviation (Three Cornered Hat)

THIS PAGE INTENTIONALLY LEFT BLANK

CONCLUSIONS

In this thesis, the theory surrounding the characterization of precision clocks and oscillators is introduced in order to derive an algorithm to compute a measure of goodness for the stability of the time scale of each clock in an ensemble.

The problem of assigning weights to each clock is faced from an operations research viewpoint by formulating a nonlinear optimization problem subjected to nonlinear constraints that are based on physical considerations.

One new algorithm to find optimal weights for an ensemble of atomic clocks is introduced, and three different measures of performance are also defined in order to be able to perform a comparison among the proposed new method and four other methods actually used in time laboratories.

A comparison shows that the proposed new method provides better values for the MOP's, and also that the variability in the three *MOP*'s is the smallest using the new method.

THIS PAGE INTENTIONALLY LEFT BLANK

LIST OF REFERENCES

[1] Hewlett Packard, Application Note 1289, *The Science of Timekeeping* by David W. Allan, Neil Ashby and Cliff Hodge. 1997

[2] Judah Levine. "Introduction to Time and Frequency Metrology". *Review of Scientific Instrument*s, Vol. 70, No. 6. 1999.

[3] IEEE Standard 1139-1999, IEEE Standard Definitions of Physical Quantities for Fundamental Frequency and Time Metrology —Random Instabilities.

[4] Stein, S. R., "Frequency and Time: Their Measurement and Characterization," *Precision Frequency Control* , Vol. 2, Academic Press, New York, pp. 191–232, 1985.

[5] David W. Allan, "Time and Frequency (Time-Domain) Characterization, Estimation and Prediction of Precision Clocks and Oscillators", *IEEE Transactions of Ultrasonics, Ferroelectrics and Frequency Control*, Vol UFFC-34, No. 6. 1987.

[6] Sullivan, D. B., Allan, D. W., Howe, D. A., and Walls, F. L., *National Institute of Standards and Technology, Technical Note 1337*, 1990.

[7] David A. Howe, David W. Allan and J. A. Barnes, "Properties of Signal Sources and Measurements methods", *Proceedings of the 35th Annual Symposium on Frequency Control*, 1981.

[8] Karstachoff P., *Frequency and Time*, Academic Press, New York 1978.

[9] David W. Allan, "Standard Terminology for Fundamental Frequency and Time Metrology", *42th Annual Frequency Control Symposium* 1988.

[10] Time and Frequency Division National Institute of Standards and Technology, "The Role of Phase Noise Research and Metrology" http://www.bldrdoc.gov/timefreq/phase/index.html, Aug 2003.

[11] David A. Howe, David W. Allan and J. A. Barnes, "Properties of Signal Sources and Measurements Methods".

http://www.bldrdoc.gov/timefreq/phase/Properties/main.htm, Aug 2003.

[12] David W. Allan and J. A. Barnes, "A modified Allan variance with Increased Oscillator Characterization Ability", *Proceedings of the 35th Annual Symposium on Frequency Control*, pp. 470-474, 1981.

[13] C. A. GreenHall, "Estimating the Modified Allan variance", *Proceedings of the IEEE International Frequency Control Symposium*, pp 346-353, 1995.

[14] David. W. Allan, "Statistics of atomic frequency standards," *Proc. IEEE,* vol. 84, July 1996.

[15] Baugh, R.A. "Frequency Modulation Analysis with the Hadamard variance", *Proceedings of the Annual Symposium on Frequency Control*, pp. 222-225, 1971.

[16] K. Wan, E. Visr and J. Roberts, "Extended variances and Autoregressive Moving Average Algorithm for the Measurement and Synthesis of Oscillator Phase Noise", *Proceedings of the 43th Annual Symposium on Frequency Control*, pp.331-335, 1989.

[17] W. J. Riley, "The Calculation of Time Domain Frequency Stability" http://home.comcast.net/~w.j.riley/paper1ht.htm, Aug 2003.

[18] F. J. Galindo, "Protagonismo de la desviación de Allan en metrología de tiempo y frecuencia", personal comunication unpublished.

[19] P. Lesage and C. Audoin, "Characterization of Frequency Stability: Uncertainty due to the Finite Number of Measurements", *IEEE Transactions on Instrumentation and Measurement*, Vol. IM2-2, pp. 157-161, 1973.

[20] A. Premoli and P. Tavella, "A revisited Three-Cornered Hat Method for Estimating Frequency Standard Instability", *IEEE Transactions on Instrumentation and Measurement*, Vol. 42, No. 1, pp. 7-13, 1993.

[21] P. Tavella and A. Premoli, "Estimating the Instabilities of *N* Clocks by Measuring Differences of their Readings", *Metrologia*, Vol 30, pp. 479-496, 1993/94.

[22] F. J. Galindo et al. “Estimation of the covariance Matrix of Individual Standards by means of Comparison Measurements”, *World Scientific,* submitted 21/02/02.

[23] P. Tavella and A. Premoli, “Characterization of Frequency Standard Instability by Estimation of Their covariance Matrix”, *Proceedings of the 23rd Annual Precise Time and Time Interval (PTTI) Applications and Planning Meeting*, pp. 265-276, 1991.

[24] F. J. Galindo and J. Palacio, “Estimating the Instabilities of *N* Correlated Clocks”, *Proceedings of the 31st Annual Precise Time and Time Interval (PTTI) Applications and Planning Meeting*, pp. 285-295, 1999.

[25] F. Torcasso et. al., “Estimating Frequency Stability and cross-correlation”, *Proceedings of the 31 Annual Precise Time and Time Interval (PTTI) Applications and Planning Meeting*, pp. 69-82, 1998.

[26] J. E. Gray and D. W. Allan, “A Method for Estimating the Frequency Stability of an Individual Oscillator”, *IEEE Proceedings of the Annual Symposium on Frequency Control*, pp. 222-225, 1974.

[27] J. A. Barnes, “Time Scales Algorithms using Kalman Filters – Insights from Simulations”, *2nd Atomic Time Scale Algorithm Symposium*., Boulder, CO, 1982.

[28] G. Marsaglia, “Diehard battery of tests of randomness, The Marsaglia random number CDROM”, *Department of Statistics, Florida State University*, http://stat.fsu.edu/pub/diehard, Sep 2003.

[29] N.J. Kasdin and T. Walter, “Discrete Simulation of Power Law Noise”, *IEEE Proceedings of the Annual Symposium on Frequency Control*, pp. 274-283, May 1992.

THIS PAGE INTENTIONALLY LEFT BLANK

INITIAL DISTRIBUTION LIST

1. Defense Technical Information Center
   Ft. Belvoir, Virginia

2. Dudley Knox Library
   Naval Postgraduate School
   Monterey, California

3. Alan Washburn
   Naval Postgraduate School
   Monterey, California

4. Paul Sánchez
   Naval Postgraduate School
   Monterey, California